Energy Conversion and Management 321 (2024) 118940

Contents lists available at ScienceDirect

Energy Conversion and Management

journal homepage: www.elsevier.com/locate/enconman

Research Paper

Synthetic natural gas as a green hydrogen carrier – Technical, economic and environmental assessment of several supply chain concepts

Fabian Carels [*], Lucas Sens, Martin Kaltschmitt

Institute of Environmental Technology and Energy Economics, Hamburg University of Technology, Eissendorfer Straße 40, 21073 Hamburg, Germany

ARTICLE INFO

Keywords:
CO_2 cycle
Green carbon
Green hydrogen
Hydrogen supply
Hydrogen supply chain assessment
Synthetic natural gas

ABSTRACT

Based on synthetic natural gas, existing natural gas markets and infrastructures can be used to make renewable sources of energy from sun- and/or wind-rich regions available on a global scale. To overcome the challenge of providing non-fossil CO_2 for the production of this synthetic natural gas, a novel concept analyzed in this paper envisages to reform the synthetic natural gas in the importing country and transporting the captured CO_2 back to the exporting country to be reused for the production of synthetic natural gas; i.e., the synthetic natural gas serves as a hydrogen carrier. This paper examines and compares the energy efficiency, cost and greenhouse gas emissions of different hydrogen supply chains using synthetic natural gas as a carrier related to the year 2030. To do so, all relevant components are taken into account to model the entire supply chains. A special focus is put on different options for providing the required CO_2 and on different technologies for synthetic natural gas reforming. The assessment shows that the availability of a cheap source of biogenic CO_2 at the point-of-export as well as electrified steam methane reforming result in the lowest hydrogen supply cost of 6.6 to 7.0 $€_{2020}/kg_{H2}$, also achieving best results in terms of energy efficiency (around 44%). With regard to minimizing greenhouse gas emissions, autothermal reforming of methane appears to be advantageous. A closed CO_2 cycle is favorable over sole onsite CO_2 provision, if no cheap CO_2 of non-fossil origin is available at the point-of-export and the costly direct air capture process would have to be used.

1. Introduction and background

International energy trading is crucial to cover the energy demand of many countries. In recent years, especially the maritime transportation of liquefied natural gas (LNG) has steadily gained significance. Thus, the volume of LNG traded worldwide almost doubled between 2010 and 2023 [1,2]. This LNG market is expected to continue to grow unabated in the coming years, particularly in light of Europe's abandonment of pipeline gas from Russia, and the sustained growth in energy demand in the People's Republic of China, one of the largest importers of LNG [3]. The dynamic growth of the LNG trade has necessitated a strong expansion of the corresponding infrastructure. For example, based on regasification terminals recently completed and currently under development, the available LNG import capacity in the European Union (EU) is expected to roughly double between 2020 and 2030 [4–6].

In parallel to these developments, the pressure to supply society with climate-neutral energy is increasing due to the obligations agreed in the Paris Climate Agreement and the more and more apparent negative and harmful consequences of climate change [7,8]. In this context, the discussion about the use of the LNG import infrastructure within a fossil-free future is being pursued with vigor, particularly within the European Union (EU). Concepts in which the LNG regasification terminals are converted to import liquefied "green" hydrogen or renewable ammonia are being discussed more frequently [9–12]. A technically simple alternative for the continued utilization of the global LNG transportation infrastructure is the development of a market for renewable synthetic natural gas (SNG) that is chemically identical to natural gas of fossil origin. Thus, SNG not only offers the opportunity to transfer existing infrastructures and markets to a fossil-free future energy system, but could also help to supply countries such as Germany, Japan or South Korea, which will likely remain dependent on energy imports for decades to come, with renewable energy [13,14].

In order to provide SNG on a systemically relevant scale, large quantities of carbon dioxide (CO_2) are required in addition to renewable ("green") hydrogen. Within an energy system that is in line with the Paris Agreement and does not release any additional greenhouse gases (GHG) into the atmosphere, the CO_2 used for SNG production must be of non-fossil origin, assuming the CO_2 is not stored underground but emitted into the atmosphere during SNG use. Due to the currently

---

* Corresponding author.
E-mail address: fabian.carels@tuhh.de (F. Carels).

https://doi.org/10.1016/j.enconman.2024.118940
Received 29 April 2024; Received in revised form 13 August 2024; Accepted 14 August 2024

Nomenclature

Abbreviation	Meaning
$ACAPEX_i$	Annuity of capital expenditures of supply chain component i, €$_{2020}$/a
AF_i	Annuity factor of supply chain component i, -
ATR	Autothermal reforming
Biog.	Biogenic carbon dioxide source
$c_{CO2\ liquefaction}$	Cost for carbon dioxide liquefaction, €$_{2020}$/kg$_{H2}$
$c_{CO2\ supply}$	Total cost for continuous carbon dioxide supply at the point-of-export, €$_{2020}$/kgH$_2$
$c_{CO2\ storage}$	Cost for carbon dioxide storage, €$_{2020}$/kg$_{H2}$
$c_{CO2\ supply,\ onsite}$	Cost for onsite carbon dioxide supply via direct air capture or biogenic source, €$_{2020}$/kg$_{H2}$
$c_{CO2\ transport}$	Cost for carbon dioxide transportation via ship, €$_{2020}$/kg$_{H2}$
$c_{component,i}$	Specific cost of the supply chain component i, €$_{2020}$/kg$_{H2}$
$c_{conversion}$	Cost for methanation and synthetic natural gas liquefaction, €$_{2020}$/kg$_{H2}$
$c_{H2\ at\ EP}$	Cost for continuous “green” hydrogen supply at the point-of-export, €$_{2020}$/kg$_{H2}$
$c_{H2\ at\ IP}$	Overall cost of hydrogen supplied at the point-of-import, €$_{2020}$/kg$_{H2}$
$c_{reconversion}$	Cost for reconversion of synthetic natural gas into compressed, purified hydrogen, €$_{2020}$/kg$_{H2}$
$c_{storage}$	Cost for synthetic natural gas storage, €$_{2020}$/kg$_{H2}$
$c_{transport}$	Cost for synthetic natural gas transportation via ship, €$_{2020}$/kg$_{H2}$
$CaCO_3$	Calcium carbonate
$CAPEX_i$	Capital expenditure of supply chain component i, €$_{2020}$
CO	Carbon monoxide
CO_2	Carbon dioxide
$CO_{2\text{-}eq}$	Carbon dioxide equivalent
DAC	Direct air capture
di	Depreciation time, a
$e_{CO2\ supply}$	Total emissions of continuous carbon dioxide supply at the point-of-export, g$_{CO2\text{-}eq}$/kg$_{H2}$
$e_{component,i}$	Emissions of supply chain component i, g$_{CO2\text{-}eq}$/kg$_{H2}$
$e_{conversion}$	Emissions from methanation and synthetic natural gas liquefaction, g$_{CO2\text{-}eq}$/kg$_{H2}$
$e_{energy,H2\ at\ EP}$	Emissions of energy use for hydrogen supply at the point-of-export, g$_{CO2\text{-}eq}$/kg$_{H2}$
$e_{energy,i}$	Emissions of supply chain component i caused by the use of energy, g$_{CO2\text{-}eq}$/kg$_{H2}$
$e_{fac,elec}$	Emission factor of a renewable electricity supply to the hydrogen production, g$_{CO2\text{-}eq}$/kW$_{hel}$
$e_{H2\ at\ EP}$	Emissions from continuous “green” hydrogen supply at the point-of-export, g$_{CO2\text{-}eq}$/kg$_{H2}$
$e_{H2\ at\ IP}$	Overall emissions of hydrogen supplied at the point-of-import, g$_{CO2\text{-}eq}$/kg$_{H2}$
$e_{leackage,i}$	Emissions of supply chain component i caused by leakage of greenhouse gases, g$_{CO2\text{-}eq}$/kg$_{H2}$
$e_{reconversion}$	Emissions from reconversion of synthetic natural gas into compressed, purified hydrogen, g$_{CO2\text{-}eq}$/kg$_{H2}$
$e_{storage}$	Emissions from liquefied synthetic natural gas storage, g$_{CO2\text{-}eq}$/kg$_{H2}$
$e_{transport}$	Emissions from synthetic natural gas transportation via ship, g$_{CO2eq}$/kg$_{H2}$
el.	Electricity
eSMR	Electrified steam methane reforming
EU	European Union
GHG	Greenhouse gas
GH_2	Gaseous hydrogen
GWP_{100}	Global warming potential for a time period over 100 years, g$_{CO2\text{-}eq}$
i	Components of the synthetic natural gas supply chain including the components of the carbon dioxide cycle
$INFL$	Projected future inflation rate, –
KOH	Potassium hydroxide
LCO_2	Liquefied carbon dioxide
LHV	Lower heating value
LNG	Liquefied natural gas
LPG	Liquefied petroleum gas
LSNG	Liquefied synthetic natural gas
LT_i	Technical lifetime supply chain component i, a
$\dot{m}_{H2\ at\ IP}$	Amount of hydrogen provided at the point-of-import, kg$_{H2}$/a
NaOH	Sodium hydroxide
NG	Natural gas
O2	Oxygen
OPEXi	Operational expenditures of supply chain component i, €$_{2020}$/a
PEM	Polymer electrolyte membrane
POX	Partial oxidation
PSA	Pressure swing adsorption
$q_{CO2\ liquefaction}$	Energy input for carbon dioxide liquefaction, kWh/kg$_{H2}$
$q_{CO2\ supply}$	Total energy input for continuous carbon dioxide supply at the point-of-export, kWh/kg$_{H2}$
$q_{CO2\ supply,\ cycle}$	Energy input for the return of carbon dioxide from the point-of-import to the point-of-export, kWh/kg$_{H2}$
$q_{CO2\ supply,\ onsite}$	Energy input for onsite carbon dioxide supply via direct air capture or biogenic source, kWh/kg$_{H2}$
$q_{CO2\ storage}$	Energy input for carbon dioxide storage, kWh/kg$_{H2}$
$q_{CO2\ transport}$	Energy input for carbon dioxide transportation via ship, kWh/kg$_{H2}$
$q_{conversion}$	Energy input for methanation and synthetic natural gas liquefaction, kWh/kg$_{H2}$
$q_{conversion\ loss}$	Energy losses during conversion from hydrogen to liquefied synthetic natural gas, kWh/kg$_{H2}$
$q_{H2\ at\ EP}$	Energy input for continuous “green” hydrogen supply at the point-of-export, kWh/kg$_{H2}$
$q_{H2\ at\ IP}$	Energy content of the hydrogen supplied at the point-of-import, kWh/kg$_{H2}$
$q_{H2\ at\ EP,\ ideal}$	Energy input at point-of-export for the supply of hydrogen effectively delivered at the point-of-import, kWh/kg$_{H2}$
$q_{H2\ SC\ losses}$	Energy input at the point-of-export to compensate losses along the supply chain, kWh/kg$_{H2}$
q_{input}	Total energy input along all supply chain components, kWh/kg$_{H2}$
$q_{reconversion}$	Energy input for reconversion of synthetic natural gas into compressed, purified hydrogen, kWh/kg$_{H2}$
$q_{reconversion\ loss}$	Energy losses during reconversion of synthetic natural gas into compressed, purified hydrogen, kWh/kg$_{H2}$
$q_{storage}$	Energy input for synthetic natural gas storage, kWh/kg$_{H2}$
$q_{storage\ loss}$	Energy losses during synthetic natural gas storage, kWh/kg$_{H2}$
$q_{transport}$	Energy input for synthetic natural gas transportation via ship, kWh/kg$_{H2}$
$q_{transport\ loss}$	Energy losses during synthetic natural gas transportation via ship, kWh/kg$_{H2}$
RWGS	Reverse water-gas shift reaction
SMR	Steam methane reforming
$WACC_{nom}$	Nominal weighted average cost of capital, –
$WACC_{real}$	Real weighted average cost of capital, –
WGS	Water-gas shift reaction
η_{SC}	Overall point-to-point hydrogen supply chain energy efficiency, %

limited and uncertain future availability of CO_2 of non-fossil origin, the implementation of technically closed CO_2 cycles is an innovative option to enable “green” energy supply chains based on SNG and other synthetic hydrocarbons [15,16].

Within such a concept, the CO_2 produced during SNG utilization would be captured and subsequently returned to the site of the “green” hydrogen production to be available there again for the generation of SNG. To enable a closed CO_2 cycle with a high overall CO_2 cycling rate, the SNG would most likely have to be used at the place of destination in large-scale units where an efficient CO_2 capturing is possible. Options for large-scale SNG application might be the use in gas-fired power plants as well as in reforming units for the provision of hydrogen. The hydrogen produced in this way could thereafter be used flexibly in various applications within the overall economy. Such a SNG-based hydrogen supply competes with other “green” hydrogen supply options (e.g., liquid hydrogen, ammonia, methanol) [17–19].

Against this background, this paper aims to provide a better understanding of SNG-based hydrogen supply while assessing novel approaches for key components of this supply chain such as the provision of CO_2 and methane reforming. Especially the CO_2 supply via a closed CO_2 cycle, as investigated in this study, represents an innovative approach that has been insufficiently addressed in the existing literature. At first, possible components of such SNG-based hydrogen supply chains and their current state of development are outlined. On this basis, potential configurations of SNG-based hydrogen supply chains are identified. Lastly, the identified supply chains are modeled and assessed related to the energy efficiency, cost and GHG emissions.

2. Hydrogen supply via SNG

Under ambient conditions, gaseous hydrogen is characterized by a very low volumetric energy density. Therefore, transportation over longer distances typically requires hydrogen conditioning to substantially enhance its volumetric energy density. This conditioning can consist of compressing or liquefying hydrogen. Here, hydrogen remains in its elementary state. In contrast, alternative options exist where hydrogen is either bound to a carrier molecule (e.g., to *Liquid Organic Hydrogen Carrier* – LOHC) or converted with another hydrogen-free molecule into a hydrogen-rich molecule (e.g., ammonia, methanol, SNG). To enable such hydrogen transportation in chemically bound forms, the respective carrier molecule must be provided at the point-of-export in addition to the hydrogen. After transportation, reconversion is necessary to supply pure hydrogen again. If hydrogen-rich molecules / hydrogen derivatives are employed for transportation, direct use may also be an option, depending on the intended end use. Fig. 1 illustrates the basic concept of supply chains for international hydrogen transportation and the above-mentioned key technical components. To allow for a fair comparison of these transportation options, this paper focuses solely on the supply of pure hydrogen, neglecting the possibility of supplying hydrogen derivatives to the end consumer.

In order to create a holistic understanding of SNG-based hydrogen supply chains, the most important system components are discussed below. In addition to an overview of the fundamental technological principles, this section also provides an insight into the current state-of-the-art of the respective technology and the potential use of existing infrastructure components.

2.1. Conversion of hydrogen to SNG

Catalytic methanation is the conversion of hydrogen to methane. The methanation reaction, also known as the Sabatier process, can be realized based on both carbon monoxide (CO) and CO_2 (equation (1) and (2)) [20]. This reaction is typically controlled by suitable catalysts (e.g., nickel, ruthenium, cobalt) [21,22].

$$CO + 3\,H_2 \rightleftharpoons CH_4 + H_2O \tag{1}$$

$$CO_2 + 4\,H_2 \rightleftharpoons CH_4 + 2\,H_2O \tag{2}$$

The two methanation reactions are interconnected through the water–gas shift reaction (WGS) (equation (3)) [20].

$$CO + H_2O \rightleftharpoons H_2 + CO_2 \tag{3}$$

Commonly, CO_2 methanation is assumed to occur in a two-step process involving the reverse water–gas shift reaction (RWGS) followed by subsequent methanation of the generated CO [23,24]. The methanation reaction is influenced in particular by temperature and pressure. For instance, within the temperature range of 250 to 550 °C, where catalytic methanation typically occurs, maintaining pressures of at least 10 bar or higher is necessary to achieve high conversion rates [25].

The methanation reaction is strongly exothermal; i.e., part of the energy bound in the educt (hydrogen) is released as heat [26]. The exploitable temperature level of this waste heat depends on the respective process design, but is likely to be at least 150 °C in large-scale systems [27]. The maximum chemical conversion efficiency describing the transfer of the energy bound in the hydrogen to the methane is 83.2 % assuming a full conversion according to equation (1) and (2). In practical applications the theoretical maximum conversion efficiency can be nearly achieved [23,25,28].

Methanation using a CO-rich synthesis gas is an established industrial process that has been employed for many decades. One example are coal gasification units, where the largest plants reach capacities within the GW scale. In contrast, methanation with CO_2 being of particular relevance for SNG-based supply of “green” hydrogen, has so far only been proven on a pilot and demonstration scale [27].

The application of this technology outside of pure research environment has been demonstrated by a plant in Werlte, Germany,

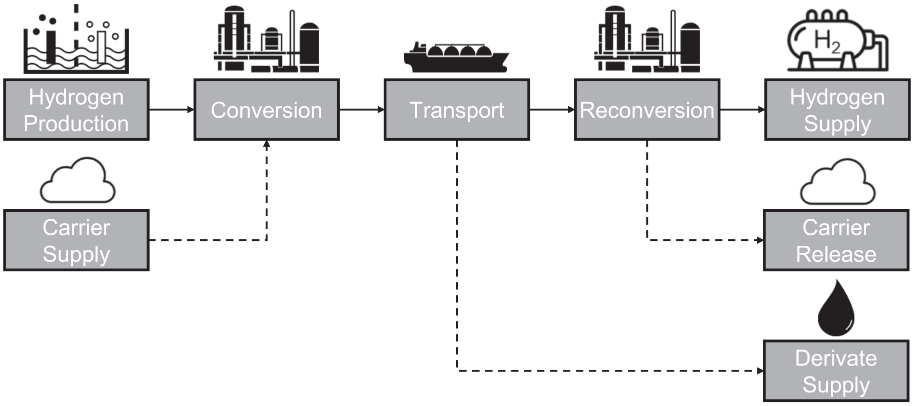

Fig. 1. Basic setup of hydrogen supply chains.

operating with a capacity of around 3.2 MW in terms of SNG output (~230 kg_{SNG}/h) [27]. Consequently, a significant upscaling of catalytic methanation would be necessary for the large-scale implementation of SNG-based international energy supply chains.

2.2. Long-distance transportation of SNG

SNG transportation over distances of several thousand kilometers can be realized via gas pipelines and LNG carriers, as is the current practice in natural gas trade. For a future international trade of hydrogen and its derivatives, especially Europe and Asia (e.g., Japan and Korea) are expected to become important importers of "green" energy [13,14]. To interconnect these import markets with regions frequently discussed as exporters of "green" energy (e.g., Arabian Peninsula, Australia, North America, Namibia), pipeline connections are often no alternative due to the distance to be covered as well as geographical or political barriers. Therefore, only ship-based transportation via liquefied synthetic natural gas (LSNG) carriers is considered here.

To enable efficient shipping, SNG is liquefied to increase the energy density by a factor of 600. The technology necessary for such a methane liquefaction is identical to the units currently applied in plants for the liquefaction of fossil natural gas. Prior to liquefaction, the SNG must be purified (i.e., all unwanted components such as water, CO_2 and nitrogen have to be removed from the synthetic methane) [29].

The liquefaction process involves a series of compression steps, heat exchanges and expansion steps to achieve a temperature below the boiling point of methane being −161.5 °C at atmospheric pressure. The SNG liquefaction process makes use of the Joule-Thomson effect of real gases according to which an expansion is accompanied by a cooling of the gas [29,30]. Energy, mainly in the form of electricity, is needed to operate such a liquefaction plant. Available data on the respective energy demand vary widely and range from 0.25 kWh/kg_{SNG} [31] to 1.39 kWh/kg_{SNG} [32].

LNG carriers are specifically designed vessels equipped with insulated cargo tanks to store LNG at cryogenic temperatures and keep it in liquid form. Due to the chemical identity, currently operated LNG carriers can also be used for the transportation of LSNG. LNG carriers under operation are usually equipped with membrane tanks or spherical tanks. Due to the better use of space and the lower weight, membrane tanks gained more and more market importance in recent years [33,34]. Especially very large LNG carriers, reaching transportation capacities of up to 266,000 m^3, are mainly equipped with membrane tanks [19,29].

During transportation, energy from the environment inevitably enters the LNG tanks, causing some of the (S)LNG to evaporate. For large LNG carriers, the boil-off rate is between 0.08 and 0.15 % per day of the transported gas. Smaller LNG carriers have typically higher boil-off rates due to the less favorable surface-to-volume ratio. Usually, the boil-off gas is used to power the ship, but re-liquefaction is also conceivable [33,35,36].

Today, natural gas is almost exclusively demanded in gaseous form. Hence, LNG is typically regasified directly at the import terminal. Also, for a hydrogen supply using SNG as a carrier, regasification at the import terminal appears to be the most suitable solution. In regasification terminals, LNG is commonly heated by seawater. The cold energy released within this process is currently not utilized in most cases. However, utilization of this cold is basically possible and could improve the overall energy efficiency of the process (e.g., electricity production in dedicated cryogenic power generation cycles, separation of gases, seawater desalination, liquefaction of other gas streams) [37].

Liquefaction plants, LNG carriers and regasification terminals have been used for decades for the intercontinental transportation of fossil LNG and are therefore available as proven technologies on a commercial scale. The future utilization of the existing LNG infrastructure for SNG supply is possible, provided that it is already available in the SNG exporting resp. importing country. However, this is not currently the case for a significant number of countries with promising potential for the production of "green" hydrogen, and thus potentially also SNG [4,32].

2.3. Reconversion of SNG to hydrogen

For hydrogen production on the basis of natural gas, steam methane reforming (SMR) is today's most commonly used process. SMR is a catalytically controlled process in which methane reacts with water vapor in a highly endothermic reaction to CO and hydrogen (equation (4)). Subsequently, a WGS is applied to oxidize the remaining CO with additional steam to CO_2 and increase the hydrogen yield (equation (5)) [38,39]. These reactions take place at temperatures between 650 and 1,000 °C and a pressure of 5 to 40 bar [40]. Further steps include hydrogen purification (e.g., pressure swing adsorption (PSA)).

$$CH_4 + H_2O \rightleftharpoons CO + 3\,H_2 \tag{4}$$

$$CO + H_2O \rightleftharpoons CO_2 + H_2 \tag{5}$$

To provide the thermal energy required for the reaction, heating of the reactor is necessary. Conventionally, SMR reactors are heated by burning additional natural gas. Typically, 30 to 40 % of the total natural gas input is used as heating fuel [41]. For SNG-based hydrogen supply involving a closed CO_2 cycle, the CO_2 created during methane reforming needs to be captured [39]. To achieve high CO_2 capture rates, the CO_2 must be captured from the syngas at the reformer outlet as well as from the flue gas of the gas burner heating the reformer. In the burner flue gas from natural gas combustion, CO_2 is found in relatively low concentrations (5 to 10 vol-%) and at low pressure, implying a high capture effort [42,43]. Accordingly, for conventional SMR equipped with CO_2 capture, which has not yet been realized on a large scale, CO_2 capture rates of maximum 90 % are reported [42,44–46].

To overcome the technical challenges associated with CO_2 capture in conventional SMR, various alternative processes are being discussed for methane reforming. Processes in which the CO_2 does not occur diluted but highly concentrated at a single point are particularly promising.

One widely discussed alternative for methane-based hydrogen production meeting these requirements is autothermal reforming (ATR) [45,47–49]. Here, the endothermic SMR (equation (4)) is combined with exothermic partial oxidation (POX) (equation (6)) to enable the reformation to be operated adiabatically (heat-tight); i.e., no heat needs to be provided externally [47]. Accordingly, CO_2 is produced exclusively in the reactor and can be captured comparatively easy. However, oxygen (O_2) must be supplied to the reaction in order to enable the POX (equation (6)) [48].

$$CH_4 + \frac{1}{2}O_2 \rightleftharpoons CO + 2\,H_2 \tag{6}$$

Existing large-scale plants applying ATR technology are typically designed to provide CO– and hydrogen-rich synthesis gases. To date, there is no large-scale experience with hydrogen production by means of ATR equipped with CO_2 capture [48]. When ATR is to be applied in the future for the production of pure hydrogen, e.g., as part of an SNG-based hydrogen supply chain, the resulting CO can be converted with water vapor within a WGS (equation (5)) to CO_2 and hydrogen, increasing the hydrogen yield. The separation and purification of the product gases (hydrogen and CO_2) can be realized by a combination of amine scrubbing and PSA [45,48]. Since all generated CO_2 occur in a high concentration stream and have to be separated from the hydrogen in the purification unit anyway, high capture rates can be achieved with, compared to conventional SMR, less effort. Thus, CO_2 capture rates of 95 % and more seem to be feasible for ATR [32,39,47,50,51]. The chemical conversion efficiency of the ATR – i.e. the share of energy bound in methane converted into energy bound in hydrogen – is between 75 and 80 % [45]. This corresponds to 3.2 to 3.0 kg_{CH4}/kg_{H2}. If the overall energy balance of the process is considered, the energy demand upstream and downstream of the actual reforming must also be taken into account. In this context, the supply of pure O_2, e.g., via an air separation unit, is of particular relevance. Furthermore, energy is also required for the separation and purification of the product gases [45].

Another approach to realize high CO_2 capture rates in hydrogen production from methane involves a modification of conventional SMR. Thus, electrically heated SMR reactors are currently being developed (electrified steam methane reforming – eSMR); a small-scale demonstration plant in Foulum, Denmark, is already under operation [52,53]. In such an eSMR reactor, the use of methane to meet the heating demand of the endothermic conversion reaction is fully omitted and the CO_2 is generated exclusively within the reforming reactor. Accordingly, CO_2 capture could be realized similar to ATR and focus on the separation from the synthesis gas at the reactor outlet [44]. CO_2 capture rates of 95 % and more are predicted to be feasible for eSMR at limited additional energy expense [39,44,54]. In addition, the deployment of the eSMR technology promises further advantages. For example, in conventional SMR process, the limited thermal conductivity between the catalyst and the reactor walls and the resulting steep temperature gradients lead to a poor utilization of the catalyst, resulting in less than 5 % of the reactor volume being used as an active zone for the conversion [55–57]. The eSMR applies electrical resistance heating direct to the catalyst and thereby overcomes these limitations leading to a significantly higher catalyst utilization. Consequently, eSMR reactors can potentially have a much smaller volume at the same hydrogen output and be operated more flexibly compared to conventional SMR reactors [55,57]. A key characteristic of the eSMR is the high potential hydrogen yield. The methane demand is estimated to be between 2.4 and 2.6 kg_{CH4}/kg_{H2} [39]. Additional, significant energy demand results from the electricity to be used primarily for reactor heating which is predicted to be between 8.6 and 9.2 kWh_{el}/kg_{H2} [44].

2.4. Carrier supply – CO_2 cycle

The return of the CO_2 to the place of the SNG production includes several steps being basically comparable to the components of a seaborne transportation of SNG. The storage density of the CO_2 captured during SNG reforming is substantially increased by liquefaction; therefore, the liquid form is preferable for efficient large-scale shipping. Various combinations of pressure and temperature between the triple point (5.18 bar, −56.6 °C) and the critical point (73.8 bar, 31.1°C) are possible for CO_2 liquefaction [58]; i.e., CO_2 cannot be in a liquid state at pressures below 5.18 bar. Liquid CO_2 is already being transported by ship today. Current CO_2 carriers, primarily operated by the food and beverage industry, attain maximum transportation capacities of approx. 1,800 t CO_2 [59]. The tanks of these ships keep the CO_2 in a liquid state at relatively high pressures (16 to 21 bar) and temperatures between −22 and −30 °C [60,61]. However, liquid CO_2 shows its maximum storage density of 1,177.9 kg/m^3 at the triple point [62]. For carriers with much higher capacities, most likely needed for an economic CO_2 shipping in the context of industrial CO_2 cycles, storage conditions should be as close as possible to the triple point to allow maximum utilization of the available cargo capacity [63,64].

Taking into account the transportation conditions described above, only tanks that can both minimize heat entry and can be pressurized are suitable for shipping of liquid CO_2. Such tanks, referred to as “semi-refrigerated” tanks, are known from shipping of liquefied petroleum gas (LPG) and ethylene; i.e., the development of large-scale CO_2 tankers may be based on the design of existing LPG and ethylene carriers [63]. The most ambitious concept for large-scale CO_2 carriers proposed so far envisages a transportation capacity of 91,000 m^3 (equals $\sim$ 105,000 t_{CO2}) [65]. The fuel consumption of a vessel of such size would be in the range of 850 kWh_{LHV}/km [61].

An additional electrical energy requirement for CO_2 recycling arises from liquefaction varying between 0.1 and 0.2 kWh/kg_{CO2} [65–67], whereby the lower bound appears feasible for newly build large-scale plants. The energy demand for loading and unloading the ship as well as for CO_2 regasification is negligible in relation to shipping and liquefaction [64].

2.5. Carrier supply – Supply of non-fossil CO_2

Both, in the context of the SNG supply chain (methanation, liquefaction, transportation, regasification) and in the cycling of CO_2, it is highly likely that small gas losses occur [64,68,69]. The respective carbon loss must be compensated – for reasons of climate protection and to maintain the supplied energy over time. To ensure a GHG-neutral and renewable energy supply, the loss compensation has to be based on non-fossil carbon. Therefore, two main options can be considered for a sustainable compensation of carbon losses:

- Feeding biogenic CO_2 into the CO_2 cycle
- Feeding atmospheric CO_2 into the CO_2 cycle

Biogenic CO_2 is released by various processes converting biomass into energy, a bio-energy carrier and/or a biomass-based raw material or product. Bioenergy processes with a substantial potential for CO_2 supply are biogas and bioethanol production as well as solid biofuel combustion. The effort of such a CO_2 capture are highly dependent on the respective source [70].

- The lowest effort arises if CO_2 from bioethanol plants is used as the gas produced during alcoholic fermentation consists almost exclusively of CO_2. Accordingly, to make CO_2 from bioethanol production available for a CO_2 cycle in the sense of the concept discussed here consists solely in compression and transportation of the gas [71].
- Biogas contains a CO_2 concentration between 40 and 45 % [72]. The separation of this CO_2 from the biogas is common practice today when biogas is upgraded to biomethane. For this purpose, various processes are available (e.g., PSA, water scrubbing, membrane processes, cryogenic processes, amine scrubbing) [72,73]. Depending on the technology used, thermal and/or electrical energy is required [74].
- Also, biomass combustion processes, for example in heating plants burning wood fuels, can be used as a source for biogenic CO_2. In conventional combustion with air, the CO_2 is diluted in the flue gas stream in concentrations between 8 and 15 vol-% [71]. Although CO_2 capture from combustion flue gases has not yet been applied for the supply of biogenic CO_2, chemical (e.g., amine scrubbing) and physical removal processes have been proven on a large scale at power plants operated with fossil fuels [72]. Compared to biogas upgrading, where similar technical processes are used, a higher energy input has to be expected due to the lower CO_2 concentrations in the flue gas [70,71].

Direct air capture (DAC) is a process that enables the direct extraction of CO_2 from the ambient air. In this process, air is fed through an absorption unit that binds the CO_2. As soon as the absorbent is saturated, the CO_2 is re-dissoluted through heat supply within a regeneration process and is afterwards available as a pure stream [26]. Currently, different DAC processes are under development varying with regard to the sorbents used, the temperature level required for redissolution and the process management. Low-temperature processes typically use amine-based sorbents and require temperatures in the range of 100 °C [75]. High-temperature DAC employs an aqueous potassium hydroxide (KOH) or sodium hydroxide (NaOH) solution to absorb CO_2; temperatures of approx. 900 °C are necessary to obtain the CO_2 that is converted into calcium carbonate ($CaCO_3$) during the process [76]. DAC technologies are already available in small scale applications today. These units are characterized by high energy demands and substantial space requirements. To capture atmospheric CO_2, between 1,500 and 2,000 kWh/t_{CO2} of thermal energy and between 250 and 450 kWh/t_{CO2} of electrical energy are needed [19,75,77]. For the supply of relevant CO_2

quantities by means of DAC, a significant upscaling of the current plant size is required in addition to further technological development, e.g., to reduce energy demands.

3. Assessment methodology

This paper aims to assess SNG-based supply of elementary, “green” hydrogen. The methodological approach follows the structure outlined in Fig. 2. Firstly, the system to be assessed is defined along with its boundaries; the definition of the hydrogen supply chains is a key part of this system description (section 4.2) and is carried out in line with the selection of sound framework assumptions (section 4.1) as well as suitable publicly available technical data (section 4.3 to 4.7). The subsequent system modelling, which is based on the selected framework assumptions and data, is divided into two stages. Initially, each single component of the supply chains is modelled on the basis of scientific laws and technical relationships using a black-box approach. Subsequently, the components are linked to each other in order to model the entire supply chain. This modelling describes mass balances (input and output streams) and energy flows along the overall supply chain. Based on this system modelling, the SNG-based hydrogen supply chains can be evaluated with regard to technical, economic and environmental criteria. The following sections describe the mathematical approach for determining these evaluation criteria.

3.1. *Technical assessment*

The energy efficiency being a main technical characteristic value describes the ratio between the energy provided by a process / process chain and the total energy expended for it. Correspondingly, the overall energy efficiency of the point-to-point hydrogen supply chain (η_{SC}) is calculated by division of the energy content of the hydrogen supplied at the point-of-import ($q_{H2\ at\ IP}$) by the total energy input along all supply chain components (q_{input}) (equation (7)). q_{input} includes all forms of energy (e.g., electrical, thermal and chemical energy), irrespective of their exergy. The lower heating value (LHV) is the reference for the energy content of the hydrogen supplied and all chemical energy carriers used along the supply chain (e.g., shipping fuel).

$$\eta_{SC} = q_{H2\ at\ IP}/q_{input} \tag{7}$$

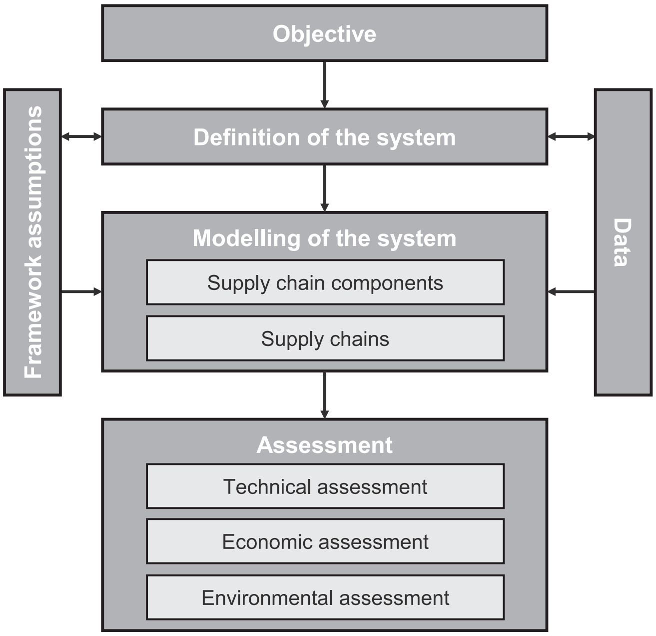

Fig. 2. General structure of the methodological approach.

The total energy input along the supply chain q_{input} is calculated as the sum of energy inputs for each component of the chain (equation (8)). These energy inputs of the specific supply chain components result from a black-box consideration and are based on literature data. Thermodynamic correlations within the individual components (e.g., during methanation) are therefore not considered in this work. $q_{H2\ at\ EP}$ defines the energy input for a continuous supply of “green” hydrogen at the methanation plant resp. the point-of-export. The energy required for a continuous CO_2 supply to the methanation plant is expressed as $q_{CO2\ supply}$. Additionally, the energy demands for methanation and SNG liquefaction ($q_{conversion}$), for LSNG transportation via ship ($q_{transport}$), LSNG storage ($q_{storage}$) and the reconversion of LSNG into compressed, purified hydrogen ($q_{reconversion}$) are considered.

$$q_{input} = q_{H2\ at\ EP} + q_{CO2\ supply} + q_{conversion} + q_{transport} + q_{storage} + q_{reconversion} \tag{8}$$

The total demand of hydrogen to be supplied to the methanation and thus the corresponding energy input for “green” hydrogen supply at the point-of-export $q_{H2\ at\ EP}$ is largely influenced by losses that occur along the supply chain (e.g., boil-off losses during transportation, (re–)conversion losses). Therefore, $q_{H2\ at\ EP}$ can be described as the sum of the energy that is needed for the supply of hydrogen effectively delivered at the point-of-import ($q_{H2\ at\ EP,\ ideal}$) and the energy required to provide additional hydrogen needed to compensate the losses along the supply chain ($q_{H2\ SC\ losses}$) (equation (9)).

$$q_{H2\ at\ EP} = q_{H2\ at\ EP,\ ideal} + q_{H2\ SC\ losses} \tag{9}$$

$q_{H2\ SC\ losses}$ includes, as summarized in equation (10), energy losses occurring during conversion from hydrogen to methane ($q_{conversion\ loss}$), during the respective reconversion via methane reforming ($q_{reconversion\ loss}$) as well as during SNG storage ($q_{storage\ loss}$) and transportation ($q_{transport\ loss}$). The latter two are mainly caused by boil-off. The conversion losses $q_{conversion\ loss}$ describe, in a simplified form, the difference between the enthalpy of the educts (hydrogen and CO_2) and the enthalpy of the product (SNG), and thus equal the heat generation during methanation. Additionally, energy losses caused by SNG leakage during its liquefaction are included in $q_{conversion\ loss}$. Correspondingly, the reconversion losses $q_{reconversion\ loss}$ are composed of the difference between the enthalpy of the SNG input and the hydrogen output of methane reforming and the hydrogen losses during final compression.

$$q_{H2\ SC\ losses} = q_{conversion\ loss} + q_{transport\ loss} + q_{storage\ loss} + q_{reconversion\ loss} \tag{10}$$

Within the scope of the supply chains considered here, the total amount of CO_2 to be supplied to the methanation plant can be divided into a part provided via a CO_2 cycle and a part additionally supplied to compensate for the occurring carbon losses. Such carbon losses can result from incomplete CO_2 capture at the reforming plant as well as from gas leakage during liquefaction, transportation and regasification of SNG and CO_2. Consequently, the total energy input for CO_2 supply ($q_{CO2\ supply}$) is calculated with equation (11).

$$q_{CO2\ supply} = q_{CO2\ supply,\ cycle} + q_{CO2\ supply,\ onsite} \tag{11}$$

A distinction is made between supply chains with and without a CO_2 cycle (further details in section 4.2). In supply chains including a CO_2 cycle, $q_{CO2\ supply,\ onsite}$ corresponds to the energy required to compensate for the carbon losses described above by means of an onsite supply of non-fossil CO_2. In supply chains without a CO_2 cycle, $q_{CO2\ supply,\ onsite}$ equals the energy required to provide the total amount of CO_2 needed for methanation via onsite supply. Correspondingly, $q_{CO2\ supply,\ cycle}$ is only relevant for supply chains including CO_2 cycling and describes the total energy demand associated with the return of the CO_2 from the point of SNG reforming to the point of methanation. According to equation (12), $q_{\mathrm{CO2\ supply,\ cycle}}$ describes the energy demand for CO_2 liquefaction ($q_{\mathrm{CO2\ liquefaction}}$), for CO_2 transportation ($q_{\mathrm{CO2\ transport}}$) and CO_2 storage ($q_{\mathrm{CO2\ storage}}$).

$$q_{\mathrm{CO2\ supply,\ cycle}} = q_{\mathrm{CO2\ liquefaction}} + q_{\mathrm{CO2\ transport}} + q_{\mathrm{CO2\ storage}} \tag{12}$$

3.2. Economic assessment

For the economic comparison of the different supply chains, the hydrogen supply cost at the point-of-import is used as the main comparative parameter. To do so, all economic assumptions and input parameters are first adjusted to the value of the euro (€) related to the year 2020 ($€_{2020}$). The subsequent method for determining the hydrogen supply cost at the point-of-import ($c_{\mathrm{H2\ at\ IP}}$) corresponds basically to the calculation of total energy input (q_{input}). Thus, $c_{\mathrm{H2\ at\ IP}}$ is the sum of the costs for all chain components, including cost for continuous hydrogen supply at the point-of-export ($c_{\mathrm{H2\ at\ EP}}$), CO_2 supply ($c_{\mathrm{CO2\ supply}}$), conversion from hydrogen to liquefied SNG ($c_{\mathrm{conversion}}$), transportation of SNG ($c_{\mathrm{transport}}$), storage of SNG (c_{storage}) and final reconversion from SNG to compressed, purified hydrogen ($c_{\mathrm{reconversion}}$) (equation (13)).

$$c_{\mathrm{H2\ at\ IP}} = c_{\mathrm{H2\ at\ EP}} + c_{\mathrm{CO2\ supply}} + c_{\mathrm{conversion}} + c_{\mathrm{transport}} + c_{\mathrm{storage}} + c_{\mathrm{reconversion}} \tag{13}$$

$c_{\mathrm{H2\ at\ EP}}$ includes the cost incurred to supply hydrogen effectively delivered at the point-of-import and hydrogen needed to compensate hydrogen losses occurring along the supply chain. According to equation (14), $c_{\mathrm{CO2\ supply}}$ includes the costs of the CO_2 cycle components and the costs of the onsite CO_2 supply required to compensate for carbon losses ($c_{\mathrm{CO2\ supply,\ onsite}}$). With regard to the cost of the CO_2 cycle, liquefaction ($c_{\mathrm{CO2\ liquefaction}}$), ship transportation ($c_{\mathrm{CO2\ transport}}$) and intermediate storage ($c_{\mathrm{CO2\ storage}}$) are taken into account.

$$c_{\mathrm{CO2\ supply}} = c_{\mathrm{CO2\ liquefaction}} + c_{\mathrm{CO2\ transport}} + c_{\mathrm{CO2\ storage}} + c_{\mathrm{CO2\ supply,\ onsite}} \tag{14}$$

The specific annual cost of the single components (i) being part of the SNG supply chain and the CO_2 cycle are calculated with equation (15). The total annual component cost is calculated by addition of the annual investment-related cost ($\mathrm{ACAPEX_i}$) and the annual operating cost ($\mathrm{OPEX_i}$). Through division by the amount of hydrogen provided at the point-of-import ($\dot{m}_{\mathrm{H2\ at\ IP}}$) the specific cost of the single component ($c_{\mathrm{component,i}}$) is obtained. In $\mathrm{OPEX_i}$, energy related costs (e.g., fuel for shipping, electricity and heat for reforming or liquefaction) as well as costs for maintenance and repair are included.

$$c_{\mathrm{component,i}} = \frac{\mathrm{ACAPEX_i} + \mathrm{OPEX_i}}{\dot{m}_{\mathrm{H2\ at\ IP}}} \tag{15}$$

By applying the annuity method, the annual investment-related cost $\mathrm{ACAPEX_i}$ can be derived from the initial investment of the respective component ($\mathrm{CAPEX_i}$) taking into account the annuity factor ($\mathrm{AF_i}$) (equation (16)).

$$\mathrm{ACAPEX_i} = \mathrm{CAPEX_i}\,\mathrm{AF_i} \tag{16}$$

The annuity factor $\mathrm{AF_i}$ is determined by equation (17). Here, the technology specific technical lifetime of the respective component ($\mathrm{LT_i}$) as depreciation period and the real weighted average cost of capital ($\mathrm{WACC_{real}}$) over that depreciation period are used.

$$\mathrm{AF_i} = \frac{\mathrm{WACC_{real}}(1 + \mathrm{WACC_{real}})^{\mathrm{LT_i}}}{(1 + \mathrm{WACC_{real}})^{\mathrm{LT_i}} - 1} \tag{17}$$

For the determination of $\mathrm{WACC_{real}}$, besides the nominal weighted average cost of capital ($\mathrm{WACC_{nom}}$), the projected future inflation rate (INFL) is also taken into account (equation (18)).

$$\mathrm{WACC_{real}} = \frac{1 + \mathrm{WACC_{nom}}}{1 + \mathrm{INFL}} \tag{18}$$

3.3. Environmental assessment

The environmental assessment of the various hydrogen supply chains is limited to the overall GHG emissions. To account different types of GHG emitted and quantify their relative impact to climate change, the global warming potential of CO_2 for a time period over 100 years ($\mathrm{GWP_{100}}$) is used as a reference [78,79]. Therefore, GHG emissions caused by each supply chain component are taken into account for calculating the overall GHG emissions of the hydrogen supply at the point-of-import ($e_{\mathrm{H2\ at\ IP}}$) (equation (19)).

$$e_{\mathrm{H2\ at\ IP}} = e_{\mathrm{H2\ at\ EP}} + e_{\mathrm{CO2\ supply}} + e_{\mathrm{conversion}} + e_{\mathrm{transport}} + e_{\mathrm{storage}} + e_{\mathrm{reconversion}} \tag{19}$$

According to equation (20), the specific GHG emissions of the chain components ($e_{\mathrm{component,i}}$) are composed of emissions caused by leakage of GHG ($e_{\mathrm{leackage,i}}$) and emissions through the use of energy ($e_{\mathrm{energy,i}}$). Emissions caused by leakage ($e_{\mathrm{leackage,i}}$) are only accounted for if they have an effective additional impact on global warming. In the concept analyzed here, only CO_2 of non-fossil origin is used to compensate for carbon losses. As a result, the CO_2 balance of the overall system is offset and there is no additional climate impact due to CO_2 leakage (e.g., through incomplete capture during methane reforming or slip during CO_2 liquefaction). This is contrasted by methane leakages (e.g., through methane slip during liquefaction or boil-off gas released to the atmosphere). While these are offset with regard to the carbon mass balance too, an additional climate impact must be considered due to the higher GHG potential of the released methane compared to the captured CO_2.

$$e_{\mathrm{component,i}} = e_{\mathrm{leackage,i}} + e_{\mathrm{energy,i}} \tag{20}$$

4. Framework, system definition and data

A fair technical, economic, and environmental assessment of SNG-based hydrogen supply chains is only possible with sound framework assumptions as well as realistic technology parameters set for the calculations. This section provides an overview of the framework defined, assumptions made and the technology parameters selected. The techno-economic data presented here and used for the system modelling is the result of comprehensive literature research. When more than two literature sources are cited for a single value, the median value of the cited sources was used.

4.1. Framework assumptions

A point-to-point supply is assumed for the evaluation of the different hydrogen supply chains. The point-of-import and −export are located in the immediate vicinity of the respective ports; i.e., international shipping is considered as the exclusive mode of transportation. The distance for shipping SNG from the point-of-export to the point-of-import and the return of CO_2 is 10,000 km; this is in line with the scale of frequently discussed [17,19,80–82] transportation routes for “green” energy (e.g., from Namibia, the Arabian Peninsula and the coast of Texas to ports in the North Sea like Rotterdam and Wilhelmshaven or also from the southern coast of Western Australia to Japan or Korea). For all examined supply chains, the supply of gaseous hydrogen with a purity $\geq 99.95\ \%$ and a pressure of 100 bar at the point-of-import is assumed.

For the calculation of the $\mathrm{WACC_{real}}$ according to equation (18), the $\mathrm{WACC_{nom}}$ is set to 8 % and the projected future inflation rate INFL to 2 % [83,84]. The reference year for all technology-specific parameters (technical, economic and environmental) is 2030. Operation with 8,000 h/a (full load) is presumed for all components downstream of the hydrogen supply at the point-of-export.

GHG emissions resulting from the construction and installation of supply chain components (e.g., PV plants, wind turbines, electrolyzers, methanation plants, ships) are not considered. This aligns with the methodology established by the European Union (EU) for assessing the GHG emissions associated with "green" hydrogen and other renewable fuels of non-biological origin (Commission Delegated Regulation (EU) 2023/1185) [85]. For the accounting of climate-impacting GHG emissions caused by gas leakage, a GWP_{100} of 25 $kg_{CO_2\text{-eq}}/kg$ is used for methane and 6 $kg_{CO_2\text{-eq}}/kg$ for hydrogen [86].

4.2. Definition of hydrogen supply chains

The technology alternatives presented in sections 2.1 to 2.5 allow various possibilities for specific configurations of SNG-based hydrogen supply chains. For the definition of the point-to-point supply chains to be assessed according to the methodology introduced in section 3, a distinction is made between different technological concepts for the following supply chain components.

- **SNG reforming – ATR/eSMR**
  While the thermal energy required for SNG reforming is provided internally when using the ATR (i.e., by using additional methane), the heat requirement for the eSMR is met externally by heating the reactor electrically.
- **Concept for CO_2 supply – With/without CO_2 cycle**
  Supply chains with and without a CO_2 cycle are taken into account. If a CO_2 cycle is used, the CO_2 source available at the point-of-export is used exclusively to cover carbon losses. If no CO_2 is returned, the entire amount of required CO_2 is provided via DAC or from a biogenic source.
- **Available CO_2 source at the point-of-export – Biogenic source/DAC**
  Supply pathways are considered that exploit a biogenic CO_2 source and pathways that extract CO_2 from ambient air by using the DAC technology.

Fig. 3 provides an overview of the SNG-based hydrogen supply chains and its main components. All possible combinations derived from the technologies discussed in section 2 result in a total of eight supply chains and are presented in Table 1. These supply chains will be assessed in this paper.

4.3. Continuous hydrogen supply at the point-of-export

A continuous "green" hydrogen feed to the methanation unit is assumed. In addition to the water electrolysis, systems for a continuous "green" hydrogen supply usually also include seawater treatment, intermediate hydrogen storage and the necessary gas compression between the electrolyzer and the storage facility. Intermediate hydrogen storage is particularly relevant given the fluctuating supply of electricity from wind power and solar radiation. The detailed modeling of such a system for continuous hydrogen supply is not realized here. Instead, literature values are used to describe the technical, economic and environmental parameters of this continuous hydrogen supply.

For a continuous "green" hydrogen supply related to the year 2030 at the point-of-export, an energy input of 50 kWh_{el}/kg_{H2} is assumed corresponding to an efficiency of around 67 % in relation to the LHV [87,88]. The cost for such a continuous hydrogen supply is set at 3.5 €/kg_{H2} (based on [87]). Neglecting any construction and installation-related emissions (section 4.1), the system for "green" hydrogen supply causes GHG emissions exclusively through leakages. It is assumed that 0.2 % of the hydrogen leaks directly into the atmosphere during production [89]. Further climate-relevant hydrogen leakages occur during compression with losses of 0.5 % [88,90].

4.4. Conversion

The production of SNG via catalytic methanation and its liquefaction are key processes for allowing the LSNG to be shipped; the respective parameters are listed in Table 2. Thus, the methanation plant achieves the maximum chemical conversion efficiency of 83.2 % (in Table 2

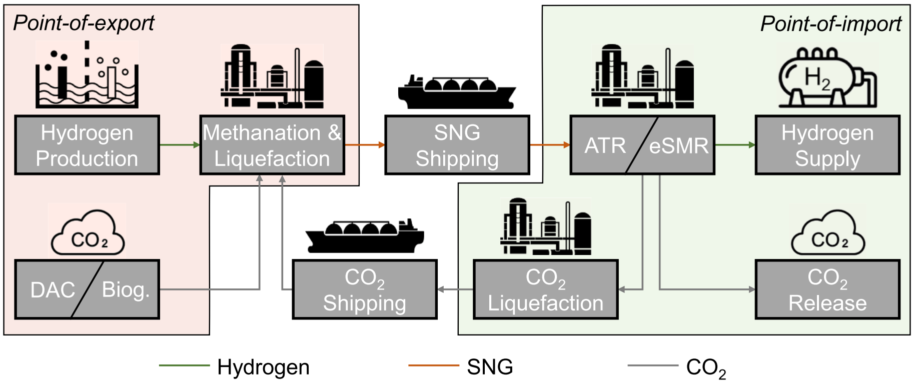

Fig. 3. SNG-based hydrogen supply chains with different technology alternatives
(ATR = Autothermal reforming; Biog. = Biogenic carbon dioxide source; CO_2 = Carbon dioxide; DAC = Direct air capture; eSMR = Electrified steam methane reforming).

Table 1
Configurations of the assessed hydrogen supply chains.

Supply Chain	Technology for SNG reforming	Concept for CO_2 supply	CO_2 source at the point-of-export
Internal Heat Supply – CO_2 Cycle – DAC	ATR	CO_2 cycle	Ambient air (via DAC)
Internal Heat Supply – CO_2 Cycle – Biogenic	ATR	CO_2 cycle	Biogenic CO_2 source
Internal Heat Supply – Onsite CO_2 Supply – DAC	ATR	CO_2 only from source at point-of-export	Ambient air (via DAC)
Internal Heat Supply – Onsite CO_2 Supply – Biogenic	ATR	CO_2 only from source at point-of-export	Biogenic CO_2 source
External Heat Supply – CO_2 Cycle – DAC	eSMR	CO_2 cycle	Ambient air (via DAC)
External Heat Supply – CO_2 Cycle – Biogenic	eSMR	CO_2 cycle	Biogenic CO_2 source
External Heat Supply – Onsite CO_2 Supply – DAC	eSMR	CO_2 only from source at point-of-export	Ambient air (via DAC)
External Heat Supply – Onsite CO_2 Supply – Biogenic	eSMR	CO_2 only from source at point-of-export	Biogenic CO_2 source

Table 2
Techno-economic parameters for methanation and SNG liquefaction.

Parameter	Unit	Methanation		SNG liquefaction	
Reference size	t_{SNG}/h	500		500	
CAPEX	$M€_{2020}$	3,600[a]	[19,24,41,66,92,93]	2,100[a]	[66,67,94–96]
OPEX	$\%_{CAPEX}/a$	4	[24,93]	4	[66]
Lifetime	a	20	[19]	25	[66]
Electricity demand	kWh_{el}/kg_{SNG}	0.28[a]	[19,41,67,91]	0.50[a]	[32,66,94–96]
Heat generation	kWh_{th}/kg_{SNG}	2.86[b]	based on [26]	0	
Usable share of heat	$\%_{Heat\ generation}$	85	based on [20]	/	
Hydrogen demand	kg_{H2}/kg_{SNG}	0.503[c]		/	
CO_2 demand	kg_{CO2}/kg_{SNG}	2.743[c]		/	
SNG loss	%	0		0.09	[68]

[a] Median value of literature data.
[b] Temperature level > 150 °C [27].
[c] Based on stoichiometrics [19,91].

depicted by the specific hydrogen and CO_2 demand) [19,91]. The energy bound in the hydrogen not converted into methane is released as heat and 85 % of that heat will be available for further use. The methane losses occurring during liquefaction are considered as leakage into the atmosphere (section 3.3).

To compensate for CO_2 losses along the CO_2 cycle or for supply chains without such a cycle, CO_2 supply at the methanation site via an onsite source can be realized by concepts utilizing biogenic CO_2 sources or with concepts applying the DAC technology (section 2.5). Table 3 shows the techno-economic parameters for CO_2 supply via DAC. A low-temperature DAC is considered allowing the integration of heat generated in methanation to cover resp. reduce the heat demand of the process. If a CO_2 supply from biogenic sources is considered, unrestricted access to CO_2 from bioethanol and plants upgrading biogas to biomethane is assumed as both processes produce a high-quality CO_2 stream as a by-product (section 2.5). Thus, for the supply of biogenic CO_2 only an additional compression energy demand of 100 kWh/t_{CO2} arises [97]. The specific cost for supplying biogenic CO_2 at the methanation site is estimated at 25 $€_{2020}/t_{CO2}$ [71].

Furthermore, methanation, SNG liquefaction and CO_2 supply can access a constant supply of renewable electricity in the case considered here. Accordingly, a high utilization of 8,000 h/a (full load) is assumed for these units. The specific cost of a baseload electricity supply largely relying on renewable energies in regions potentially exporting “green” energy is set at 0.07 $€_{2020}/kWh$ for the reference year 2030 [98]. The same specific cost is also assumed for a constant heat supply, which may be necessary to meet the thermal energy demand of the DAC unit not covered by methanation waste heat. The use of baseload electricity and heat is associated with GHG emissions of around 40 $g_{CO2\text{-}eq}/kWh$.

Table 3
Techno-economic parameter for CO_2 supply via low-temperature DAC.

Parameter	Unit	Low-temperature DAC	
Reference size	t_{CO2}/h	150	
CAPEX	$M€_{2020}$	830	[77]
OPEX	$\%_{CAPEX}/a$	4	[77]
Lifetime	a	25	[77]
Electricity demand	kWh_{el}/kg_{CO2}	0.25	[19,77]
Heat demand	kWh_{th}/kg_{CO2}	1.5[a]	[19,77]

[a] Heat demand before integration of methanation heat; Temperature level ~ 100 °C[75].

4.5. Ship transportation

The assumed parameters for SNG import by ship and the respective return of the CO_2 are shown in Table 4. The boil-off gas (BOG) generated during transportation is sufficient to power the LNG carrier, ensuring that no additional marine fuel supply is required. The LNG carrier is equipped with a contemporary two-stroke dual-fuel engine, where 0.18 % of the

Table 4
Techno-economic parameter for LSNG and LCO_2 carrier.

Parameter	Unit	LSNG carrier		LCO_2 carrier	
Reference size	m^3	266,000	[19]	91,000	[65]
Payload	t_{SNG} resp. t_{CO2}	120,000[a]		105,000[d]	
CAPEX	$M€_{2020}$	200	[19]	111	based on [63]
OPEX	$\%_{CAPEX}/a$	3	[19]	5	[61,92]
Lifetime	a	30	[19]	30	based on [19]
Average speed	km/h	30	based on [19]	30	[64]
Fuel demand	kWh_{fuel}/km	0[b]		830	[61]
Boil-off rate	$\%_{Load}/d$	0.15	[94,96]	0.15	[65,100]
Engine slip	$\%_{BOG}$	0.18	[69,99]	/	
Flash rate	$\%_{Load}$	0.13	[68]	0.13	based on [68,100]
Recovery rate flash	$\%_{Flash}$	95	[68]	95	based on [68,100]
Un/Loading time	h/transfer	96	[c]	45	based on [61,64]
Operating cost	$€_{2020}/h$	572	based on [101]	572	based on [101]
Harbor fees	$€_{2020}$/transfer	260,000	[c]	60,000	[61]
Utilization	h/a	8,000	[102]	8,000	[102]

[a] Storage density of 450 kg/m^3 assumed.
[b] Use of boil-off gas as fuel assumed, sufficient to meet energy demand of roundtrip.
[c] Value based on personal information from industry.
[d] Storage density of 1,150 kg/m^3 assumed.

BOG is released unburned as slip gas [69,99]. The flash rate describes the generation of additional BOG during the loading and unloading of tanks with cryogenic liquids. For capturing and recovering the BOG generated as flash during loading and unloading of the LNG carrier, a rate of 95 % is assumed [78]. At the port-of-export, this recovery involves the return to the SNG liquefaction plant; at the port-of-import, the BOG from the flash can be used directly in the reforming unit (ATR or eSMR).

At present, there is no empirical data available regarding the generation of BOG during the large-scale transportation of liquid CO_2 (LCO_2) by ship. Thus, it is assumed that the boil-off rate for LCO_2 carriers as well as the flash and recovery rates do not differ significantly from that of LNG carriers [100]. However, an additional shipping fuel must be provided to power the LCO_2 carrier. A renewable fuel is considered, with costs of 0.11 $€_{2020}/kWh_{LHV}$ and emissions of 85 g_{CO2}/kWh_{LHV}. There is no reliquefaction of the CO_2 occurring as boil-off during transportation.

4.6. Storage

In order to balance the intermittent loading and unloading of ships with the near-continuous operation of the up- and downstream components, storage of LSNG and LCO_2 is necessary. Table 5 summarizes the techno-economic parameters considered for these storage systems. To determine the reference size of the storage systems a capacity equal to the ship's payload is assumed (storage factor of 1) [63]. The assumptions regarding the specific boil-off rates during LSNG and LCO_2 storage align with those applied to ship transportation. However, as the storage tanks under consideration are stationary systems in the immediate vicinity of the respective up- and downstream components, BOG recovery of 95 % is feasible [78]. The recovered BOG is either returned to the liquefaction or used directly in methanation (in the case of LCO_2 storage at point-of-export) resp. reforming (in the case of LSNG storage at point-of-import).

4.7. Reconversion

Table 6 lists the techno-economic parameters of the reforming technologies considered for SNG reconversion into hydrogen and CO_2. In order to ensure maximum CO_2 concentration in the product gas stream, ATR operation with pure O_2 is assumed. An air separation unit is considered to supply the required O_2. The supplementary electrical energy demand of the ATR includes electricity required for the separation of the product gases (hydrogen and CO_2) and other auxiliary units. In the case of the eSMR, the electricity required to externally heat the reactor is added.

After the SNG has been reformed, the produced hydrogen must be compressed to the targeted pressure level of 100 bar. In addition, the captured CO_2 must be liquefied to enable it's shipping. Table 7 shows the techno-economic parameters of hydrogen compression and CO_2 liquefaction. Gas losses are not captured and leak directly into the atmosphere.

In line with the considerations for the export country, a constant

Table 5
Techno-economic parameter for LSNG and LCO_2 storage tanks.

Parameter	Unit	LSNG storage tank		LCO_2 storage tank	
Reference size	m^3	266,000[a]		91,000[a]	
CAPEX	$M€_{2020}$	540[b]	[95,103]	250[b]	[63,104]
OPEX	$\%_{CAPEX}/a$	2	[17]	5	[58,63]
Lifetime	a	30	[95]	30	based on [95]
Boil-Off rate	%/d	0.05	[68]	0.05	based on [68]
Recovery rate boil-off	$\%_{BOG}$	95	[68]	95	based on [68]
Average storage time	d	10[c]	own assumption	4[c]	own assumption

[a] According to carrier payload.
[b] Median value of literature data.
[c] Deviating storage times result from a different number of ships – since fewer ships are needed, longer, de/loading-free periods to be bridged by storage arise for SNG.

Table 6
Techno-economic parameter for reconversion of SNG to hydrogen via ATR and eSMR.

Parameter	Unit	ATR		eSMR	
Reference size	t_{H2}/h	200		200	
CAPEX	$M€_{2020}$	4,800[a]	[39,45,50,51,92]	2,900[a]	[39,44]
OPEX	$\%_{CAPEX}/a$	4	based on [39,51]	4	based on [39,44]
Lifetime	a	25	[45]	25	[39,44]
Methane demand	kg_{SNG}/kg_{H2}	3.1[a]	[39,45,50,92]	2.5[a]	[39,44]
Electricity demand	kWh_{el}/kg_{H2}	1.9[a]	[39,45,50]	8.9	[39,44]
O_2 demand	kg_{O2}/kg_{H2}	3.1[b]		/	
O_2 supply			based on [17,105–108]		
Electricity demand	kWh_{el}/kg_{O2}	0.29		/	
Cost	$€_{2020}/kg_{O2}$	0.08		/	
CO_2 capture rate	%	95[a]	[39,45,50,51,92]	95[c]	
Outlet pressure	bar	30	based on [38,45]	30	based on [38,45]

[a] Median value of literature data.
[b] Based on stoichiometrics for the stated methane demand.
[c] assumed to be identical to ATR, since requirements for CO_2 capture seem to be similar.

Table 7
Techno-economic parameter for hydrogen compression and CO_2 liquefaction.

Parameter	Unit	Hydrogen compression		CO_2 liquefaction	
Reference size	t_{H2}/h resp. t_{CO2}/h	200		1,500	
CAPEX	$M€_{2020}$	192[b]	[88,90,109]	430[b]	[58,63]
OPEX	$\%_{CAPEX}/a$	5	[88,90]	4	[63]
Lifetime	a	15	based on [88,90]	25	[17]
Electricity demand[a]	kWh_{el}/kg_{H2} resp. kWh_{el}/kg_{CO2}	0.6	based on [90,110,111]	0.12[b]	[17,58,63,65,97]
Hydrogen resp. CO_2 loss	%	0.5	[88,90]	0.1[c]	based on [68]

[a] For compression resp. liquefaction based on gas at 30 bar (outlet pressure of reforming).
[b] Median value of literature data.
[c] Assumed to be identical to SNG liquefaction.

electricity supply is also assumed for SNG reforming, final hydrogen compression and CO_2 liquefaction. Costs of 0.1 $€_{2020}$/kWh are considered for the supply of baseload electricity in 2030 in regions which are expected to become import hubs for hydrogen (mainly Europe and East Asia) [80]. 85 g_{CO2-eq}/kWh_{el} is assumed for the emission intensity of this baseload electricity supply (based on [112,113]).

5. Results and discussion

In the following, the results of the hydrogen supply chain assessment are discussed. The results are based on a supply chain modeling according to the methodological approach introduced in section 3 and the data and assumptions set out in section 4. Fig. 4 shows the energy input, cost and GHG emissions for a SNG-based supply of elementary, gaseous hydrogen at 100 bar.

5.1. Energy input and hydrogen supply chain efficiency

The total energy input for the supply of one kWh_{LHV} of hydrogen at the point-of-import ranges from 2.3 to 2.8 kWh, resulting in an overall energy efficiency between 36 and 44 %. The majority (80 to 90 %) of the energy demand is dedicated to hydrogen production at the point-of-export. While the choice of the CO_2 supply option has only a minor impact on the overall supply chain efficiency, the reforming technology exerts a more substantial influence. Thus, supply chains employing eSMR (i.e., meeting the heating demand of the reforming externally through additional electricity) are around five percentage points more efficient than those using ATR (i.e., meeting the heating demand of the reforming internally through consumption of additional methane). The reason is that the chemical reconversion efficiency (energy in methane to energy in hydrogen) of eSMR is clearly higher compared to ATR (Table 6). Accordingly, in supply chains with ATR considerably more SNG – and therefore more hydrogen – must be produced at the point-of-export to supply the same amount of hydrogen at the point-of-import. Due to this, in cases with ATR the energy input to compensate for the supply chain losses (*H_2 Production – Only Losses*) is about twice as high as in cases with eSMR, as shown in Fig. 4. The more efficient methane utilization in supply chains with eSMR goes hand in hand with an additional energy demand at the point-of-import for heat supply (*Reconversion – Only Heat Supply*). Overall, however, this form of external heat supply is more energy–efficient in the scenario under consideration than supply chains with ATR where additional methane is used to provide the heat internally.

With regard to the different CO_2 supply options considered, Fig. 4 shows that CO_2 supply using only a local biogenic source is most efficient and requires hardly any energy input relevant for the overall efficiency. This result is essentially based on the assumption that high-purity CO_2 is available, which only needs to be compressed for methanation (section 4.4). The supply of the entire CO_2 demand via DAC leads to a drop in total efficiency of around three percentage points compared to the sole use of biogenic CO_2. The energy demand of DAC-based CO_2 supply can be reduced by around two thirds through the implementation of a cycle. Taking into account the assumptions made regarding the CO_2 capture rate at the SNG reforming plant and other carbon losses (e.g., boil-off losses in the form of CO_2 and methane), around 90 % of the CO_2 required for methanation can be provided via the cycle. Given this high recycling rate, it is of secondary importance for the energy efficiency of supply chains with a CO_2 cycle whether the carbon losses are compensated by means of DAC or from a biogenic source. This is particularly true as the DAC's heat demand can be completely covered by methanation waste heat if the majority of the CO_2 is supplied via a cycle. This methanation heat is not sufficient to cover the many times higher heat demand of a CO_2 supply solely via DAC. Accordingly, the provision of additional heat (from external sources) is necessary in this case.

5.2. Hydrogen supply cost

The hydrogen supply costs in the considered pathways range between 6.6 and 8.6 $€_{2020}/kg_{H2}$, as shown in Fig. 4. The composition of the costs largely corresponds to that of energy input. The hydrogen production has a predominant influence, accounting for 60 to 75 % of overall supply cost. Beyond hydrogen production, conversion (includes methanation and liquefaction), CO_2 supply, and reconversion contribute notably to the hydrogen supply cost, whereas SNG storage, SNG ship transportation, and hydrogen compression have only a marginal impact. Related to the costs of SNG transportation, a provision of shipping fuel via boil-off gas was assumed. Therefore, in Fig. 4 shipping fuel costs (as well as energy demand and GHG emissions) appear as part of *H_2 Production – Only Losses*.

The use of eSMR for reconversion leads to a reduction of total supply cost of about 1 $€_{2020}/kg_{H2}$ compared to reconversion by means of ATR. As with the energy input (section 5.1), the higher chemical conversion efficiency of the eSMR reduces the cost of producing additional hydrogen to compensate for supply chain losses (*H_2 Production – Only Losses*) by more than half. Further advantages for supply chains characterized by high chemical conversion efficiencies arise because fewer material flows (SNG and CO_2) have to be liquefied, transported and temporarily stored in order to provide the same amount of hydrogen. For example, in supply chains with reconversion via eSMR, the components of the transportation chain can be dimensioned considerably smaller (e.g., capacity of the liquefaction plants, number of ships) – and thus the overall costs can be reduced – compared to chains with reconversion via ATR. Under the assumptions made, the outlined cost benefits of the supply chains with eSMR outweigh the additional costs of providing the reconversion heat via electricity (*Reconversion – Only Heat Supply*).

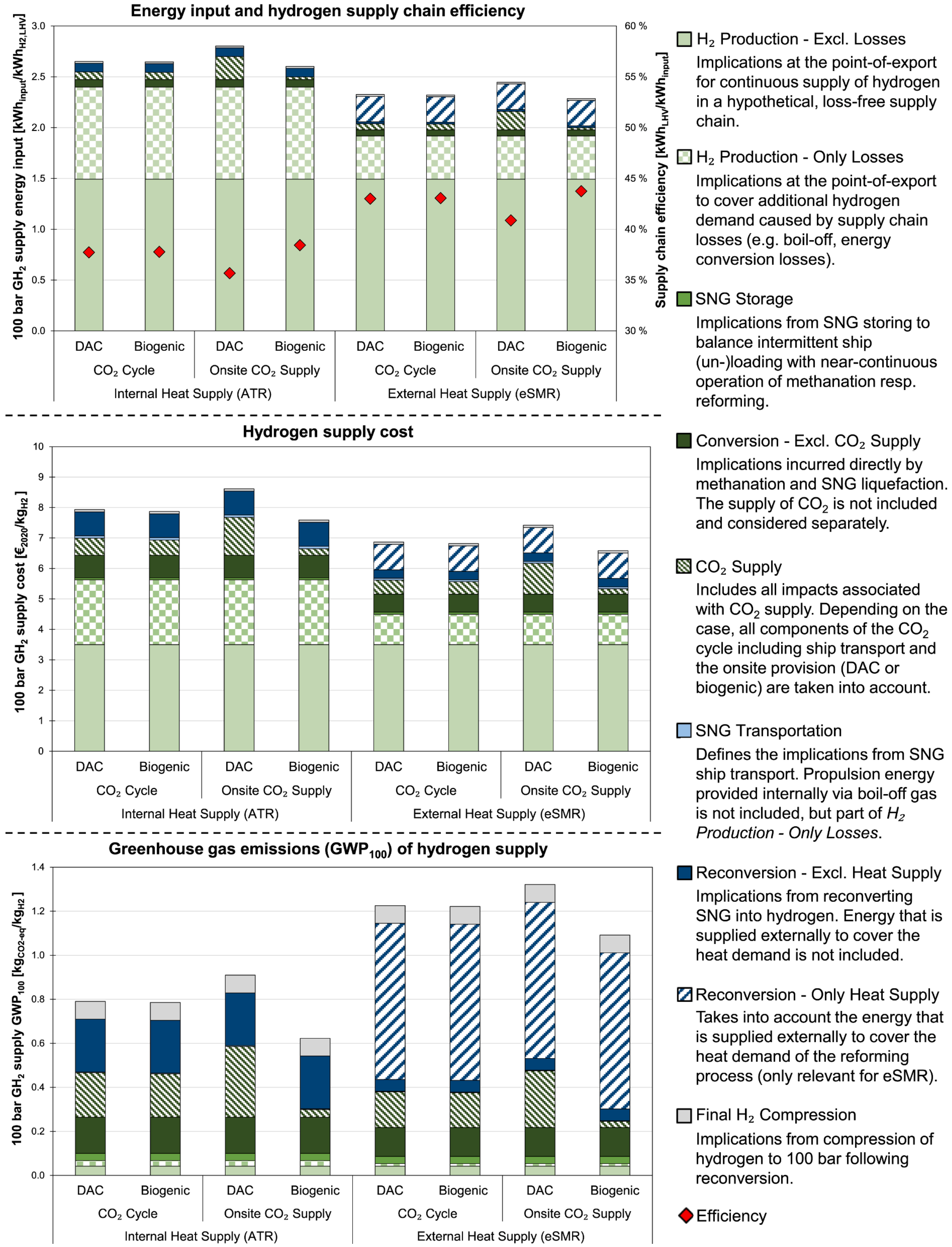

Fig. 4. Energy input and efficiency (top), cost (center) and GWP_{100} (bottom) in 2030 for a SNG-based supply of gaseous hydrogen at 100 bar (ATR = Autothermal reforming; DAC = Direct air capture; eSMR = electrified steam methane reforming; GH_2 = Gaseous hydrogen; GWP_{100} = Global warming potential for a time period over 100 years; LHV = Lower heating value, SNG = Synthetic natural gas).

Among the CO_2 supply options considered, supply chains utilizing a biogenic CO_2 source show the lowest costs, whereas supply exclusively via DAC leads to the highest costs. By implementing a CO_2 cycle, the CO_2 supply cost are more than halved compared to the sole use of DAC systems; this leads to a reduction of the resulting hydrogen supply cost of approx. 0.7 $€_{2020}/kg_{H2}$ (if ATR is used for reconversion, for cases with eSMR slightly lower). Under the assumptions made, the overall costs of CO_2 cycling are around 60 $€_{2020}/t_{CO2}$. At 40 $€_{2020}/t_{CO2}$, ship transportation is responsible for the majority of these costs, followed by the liquefaction with around 15 €$_{2020}$/t$_{CO2}$. The costs of the CO_2 cycle may be further reduced through the deployment of multi-gas carriers (transportation of LSNG and LCO_2 in the same ship) and the integration of SNG regasification cold into CO_2 liquefaction (these options were not assessed here). At 100 €$_{2020}$/t$_{CO2}$, the specific costs for CO_2 loss compensation using DAC are four times higher than the assumed costs for the supply from a biogenic source (section 4.1). Due to the high share of circulated CO_2 (~90 %), the availability of a biogenic CO_2 source has only little influence on the hydrogen supply cost if a CO_2 cycle is used.

For supply chains without such a cycle and with CO_2 supply exclusively onsite, the influence of biogenic CO_2 availability on the resulting hydrogen supply cost is significant. In that case, the DAC-based CO_2 supply incurs additional costs of 1 €$_{2020}$ (ATR case) resp. 0.85 €$_{2020}$ (eSMR case) per kg of hydrogen supplied at the point-of-import. As mentioned in section 5.1, in supply chains without a CO_2 cycle additional heat must be provided to cover the demand of the DAC. Thus, the specific cost for CO_2 supply by means of DAC is around 40 % higher when no CO_2 cycle is implemented (~140 €$_{2020}$/kg$_{CO2}$) compared to the previously discussed case (~100 €$_{2020}$/kg$_{CO2}$), where DAC is only used to compensate for carbon losses.

Against the background of the decisive importance of economic efficiency for a potential realization of SNG-based hydrogen supply, the sensitivity of the supply cost to a parameter variation is investigated. The aim of this parameter variation is to map a broad variety of possible supply scenarios. Therefore, parameters are varied that are largely determined by the export and import regions and/or are significantly influenced by future techno-economic developments. To do so, the following parameters are assessed:

- Hydrogen production cost at the point-of-export
- Electricity cost at the point-of-import
- Transportation distance
- CO_2 supply cost at the point-of-export

For the variation the hydrogen production cost, electricity cost and transportation distance, no distinction between different CO_2 supply options is made; instead, a general onsite CO_2 supply cost of 25 €$_{2020}$/t$_{CO2}$ is assumed. The influence of different point-of-export CO_2 cost on the resulting hydrogen supply cost is assessed separately by the variation of the corresponding parameter.

Fig. 5 shows the results of the parameter variation. It is apparent that a change in the point-of-export hydrogen production cost has a particularly strong influence on the resulting hydrogen supply cost. This impact of hydrogen production cost is slightly higher if the ATR is used to reconvert the SNG into hydrogen. The reason is that in the ATR the reforming heat is supplied internally and thus ultimately via additional hydrogen production at the point-of-export. If the eSMR is applied, the

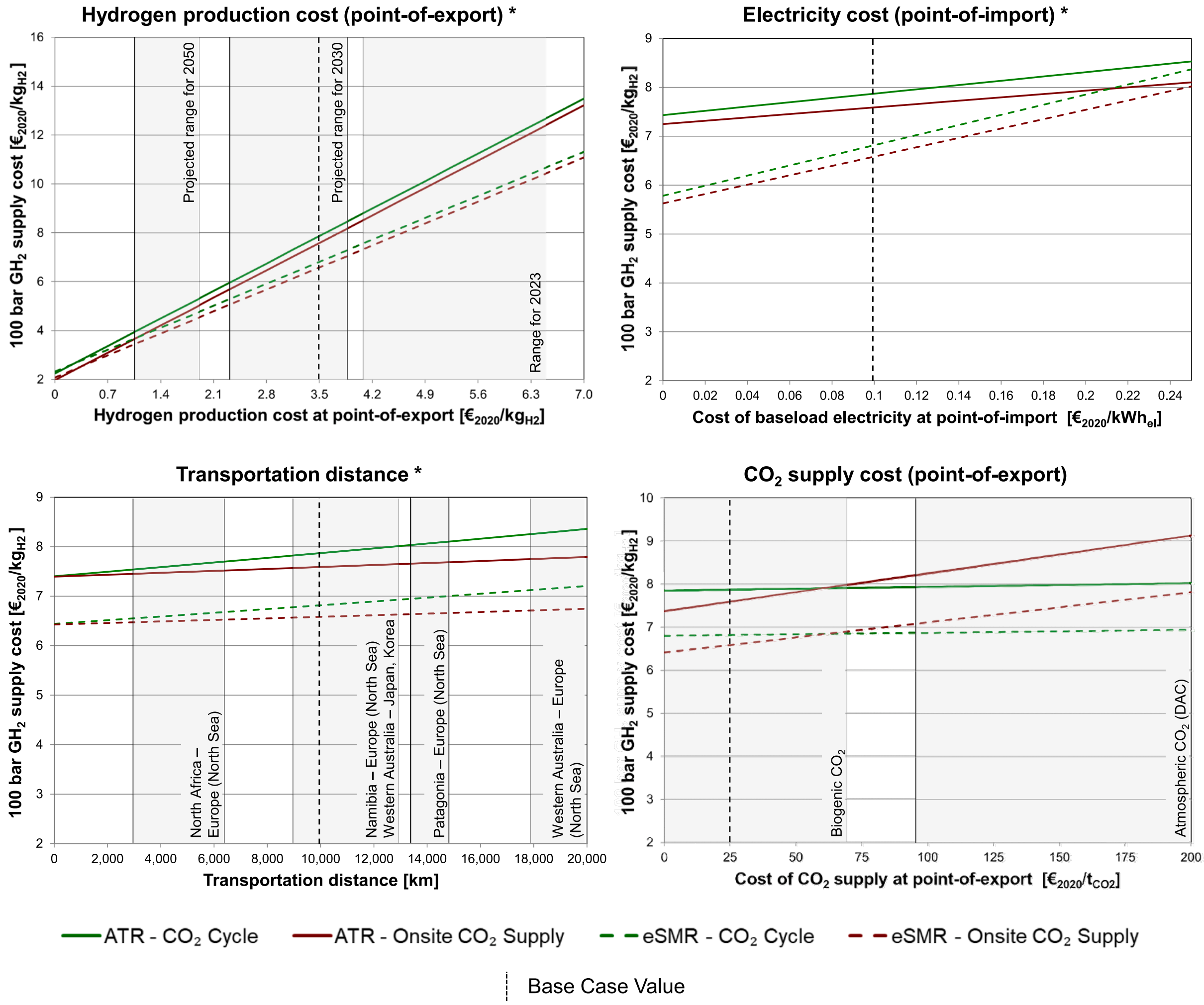

Fig. 5. Cost in 2030 for a SNG-based supply of gaseous hydrogen at 100 bar over variation of selected parameter
* 25 €$_{2020}$/t$_{CO2}$ assumed for CO_2 supply at point-of-export
(ATR = Autothermal reforming; DAC = Direct air capture; el = Electricity; eSMR = electrified steam methane reforming; GH_2 = Gaseous hydrogen; LHV = Lower heating value).

reforming heat is supplied by external electricity, resulting in a lower overall hydrogen demand and thus a lower dependence on its production cost. Furthermore, the variation in hydrogen production cost shows that the costs caused by transportation and the associated conditioning are around 2 $€_{2020}/kg_{H2}$. Since the onsite CO_2 supply cost (25 $€_{2020}/t_{CO2}$) assumed in the scenario presented in Fig. 5 are lower than the specific CO_2 recycling cost (~60 $€_{2020}/t_{CO2}$), the pathways with a CO_2 cycle have slightly higher transportation-related costs than those with onsite supply. With regard to the influence of the electricity cost at the point-of-import, the results paint a contrary picture. Thus, due to their higher energy demand at the point-of-import the hydrogen supply cost of eSMR pathways show a higher dependency on the electricity cost than pathways with ATR. Moreover, supply pathways with a CO_2 cycle are marginally more sensitive to the point-of-import electricity cost due to the additional electricity consumption of CO_2 liquefaction. In summary, the choice between ATR and eSMR is mainly influenced by the difference in energy cost in the export and import region. Basically, the eSMR has advantages due to its higher overall efficiency. However, export scenarios in which hydrogen production in the export region is very cheap and the electricity supply in the import region is very expensive are favorable for the ATR, as energy is almost exclusively consumed at the point-of-export here. Here, the more efficient utilization of the produced hydrogen by eSMR is less impactful on the overall hydrogen supply cost. For example, in a hypothetical scenario in which hydrogen could be produced at the point-of-export for 1.5 $€_{2020}/kg_{H2}$, the cost parity between supply pathways with eSMR and ATR would be given at point-of-import electricity cost of around 0.17 $€_{2020}/kWh_{el}$.

The lower charts of Fig. 5 illustrate the influence of the transportation distance and the point-of-export CO_2 supply cost on the overall hydrogen supply cost. While the two parameters discussed in the previous paragraph mainly determine the cost difference between pathways with different SNG reforming technologies, the transportation distance and the CO_2 cost primarily affect whether the use of a CO_2 cycle is beneficial. In terms of transportation distance, the influence on the hydrogen supply cost is generally rather low. For example, doubling the distance of 10,000 km assumed in the base case only results in an increase in supply cost of less than 0.5 $€_{2020}/kg_{H2}$ across all considered pathways. Supply pathways that do not involve a CO_2 cycle have a particularly low dependency on transportation distance. If a CO_2 cycle is implemented, the CO_2 transportation adds additional distance-related cost parameters (number of CO_2 carrier required, fuel consumption), resulting in a slightly higher sensitivity. The point-of-export CO_2 supply cost have hardly any influence on the hydrogen supply cost of pathways with a CO_2 cycle under the given assumptions (the CO_2 recycle rate calculated to around 90 % is particularly important here). However, if CO_2 recycling is not used, high point-of-export CO_2 cost result in high hydrogen supply cost. For a CO_2 cost of 200 $€_{2020}/t_{CO2}$, for example, the savings that can be realized through the CO_2 cycle are around 1 $€_{2020}/kg_{H2}$. It can be concluded that the cost advantages or disadvantages of implementing a CO_2 cycle are always decisively influenced by the transportation distance and the CO_2 cost at the point-of-export. For example, the cost parity between supply pathways with and without a CO_2 cycle for a transportation distance of 3,000 km is around 40 $€_{2020}/t_{CO2}$. If the distance were 20,000 km, as would be the case for exporting SNG from Australia to Europe, the CO_2 costs at the point-of-export would have to exceed 120 $€_{2020}/t_{CO2}$ to make a CO_2 cycle economically advantageous.

5.3. Greenhouse gas emissions of hydrogen supply

As Fig. 4 illustrates, the GHG emissions across the evaluated supply chains range from 0.6 to 1.3 kg_{CO2-eq}/kg_{H2}. In the considered framework, GHG emissions from hydrogen supply predominantly stem from baseload energy consumption during conversion from hydrogen to methane, CO_2 provision, and reconversion processes. Leakage-related emissions, accounting for 15 to 30 % of overall emissions, are mainly caused by hydrogen production, initial and final hydrogen compression as well as methane liquefaction. However, the sensitivity to the selected technology data is high. If, for example, a leakage rate of 1.5 % (corresponds to the range used by [66,96]) were assumed for methane liquefaction instead of 0.1 % ([68], see Table 2), the share of leakage-related emissions would rise to above 50 % while total emissions would increase to a range between 1.6 and 2.1 kg_{CO2-eq}/kg_{H2}. Furthermore, it is also conceivable that, for example due to technical reasons, the boil-off gas occurring on the LSNG tanker is not burned almost completely as assumed, but escapes into the atmosphere unused in parts. In this case, SNG transportation would become an additional relevant source of leakage-related emissions.

Notably, the level of GHG emissions is primarily influenced by the choice of reforming technologies, with supply chains using ATR demonstrating superior environmental performance with lower total GHG emissions compared to those using eSMR, despite the latter's higher energy efficiency. Thus, using ATR can reduce total emissions in the supply chains studied by 30–45 %. The higher overall energy efficiency of supply chains with eSMR has no decisive influence on the overall GHG emissions. Based on the assumption that the GHG emissions from hydrogen supply at the point-of-export are caused exclusively by leakage and are therefore comparatively low (section 4.3), the increased hydrogen losses from reconversion via ATR only lead to slight additional emissions. This is contrasted by the additional demand of baseload electricity by eSMR (*Reconversion – Only Heat Supply*), which, as assumed here, has potentially high specific emissions (section 4.7). If hydrogen supply at the point-of-export were to be accounted with higher specific GHG emissions, for example by taking into account the upstream emissions of renewable electricity generation, the different overall efficiency of supply chains with ATR and eSMR could have a noteworthy impact on the total GHG emissions. Thus, as already shown with regard to the costs, the emissions assessment is also largely dependent of the difference between emissions of energy supply in the import and export region. Low-emission hydrogen supply in export regions favors ATR-based supply chains, whereas eSMR benefits from cleaner electricity in import regions.

In the scenario under consideration, CO_2 cycling can save emissions compared to onsite CO_2 supply by means of DAC, as shown in Fig. 4. This is true, although the energy used for the CO_2 cycle (mainly electricity for CO_2 liquefaction at the point-of-import and renewable shipping fuel) has, based on the assumptions made, significantly higher specific emissions than the baseload electricity and heat used for DAC. However, this systemic advantage is outweighed by the many times higher total energy demand of the DAC compared to the CO_2 cycle (section 5.1).

6. Conclusion

The goal of this paper is to assess elementary hydrogen supply by using SNG as a carrier for "green" hydrogen. As part of this assessment, novel approaches for the provision of the required CO_2 as well as the reforming of methane to hydrogen are being investigated. To achieve this, this work evaluates the energy efficiency, cost, and GHG emissions of various supply concepts for the year 2030. The analysis of the technology components part of such supply chains illustrates that, from a technical point of view, hydrogen supply using SNG as a carrier can be a valid alternative to other ship-based hydrogen supply chains based on, e.g., ammonia, methanol or LOHC. Existing infrastructures and established technologies can be used for certain components of SNG-based hydrogen supply chains. However, there are significant technical challenges to overcome for a full-scale implementation. In particular, the catalytic methanation of hydrogen and CO_2 as well as methane reforming for the supply of pure hydrogen with a simultaneous capture of CO_2 have not yet been realized on a large scale. Also, for the supply of large quantities of non–fossil CO_2, technological innovations and/or a substantial scale-up of the current status quo may be necessary, especially if biogenic sources are not or not in the required quantity available at the point-of-export.

For a hydrogen supply based on SNG as a carrier, various supply pathways are defined, which differ in terms of the CO_2 supply option and the technical approach for the SNG reforming. Overall, the following conclusions can be drawn from the comparison of these supply pathways.

- The energy efficiency of SNG-based hydrogen supply, summing up to 36 to 44 % in the investigated pathways, is largely determined by hydrogen production at the point-of-export. The amount of hydrogen that has to be produced at the point-of-export, in turn, is clearly influenced by the supply chain losses to be compensated. Accordingly, the realization of a highly efficient energy conversion (electrolysis, methanation, SNG reforming) and low-loss energy transportation (e.g., boil-off) are essential for a SNG-based hydrogen supply with a high overall energy efficiency.
- For the evaluated concepts, the hydrogen supply cost varies between 6.6 and 8.6 $€_{2020}/kg_{H2}$ related to the year 2030. This cost of SNG-based hydrogen supply is significantly affected by hydrogen production at the point-of-export and thus by the supply chain losses.
- Under the framework assumptions considered here, the climate-impacting GHG emissions from SNG-based hydrogen supply result largely from baseload energy use along the supply chain. Accordingly, the specific emissions of the electricity and heat used for methanation, SNG liquefaction, CO_2 supply and SNG reforming are of major importance for the overall emissions of such a hydrogen supply, which are between 0.6 and 1.3 $kg_{CO2\text{-}eq}/kg_{H2}$. However, this order of magnitude is only valid assuming that barely any gas leakages occur along the SNG transportation chain. Thus, the release of just 1.5 % of the produced SNG into the atmosphere (for example in the course of liquefaction or as boil-off during transportation) would lead to a substantial increase in GHG emissions.
- As part of the supply pathways comparison, ATR and eSMR are being investigated – two processes that enable high CO_2 capture rates during reconversion of SNG into hydrogen. This assessment shows that the eSMR is generally advantageous and allows a reduction of hydrogen supply cost by 10 to 20 % due to the more efficient utilization of the SNG; i.e., if the eSMR is used, less SNG is required to provide the same amount of hydrogen. Accordingly, less hydrogen needs to be produced at the point-of-export and, consequently, all downstream components of the supply chain can be dimensioned smaller. However, scenarios are conceivable in which systemic framework conditions for hydrogen imports arise that favor SNG reconversion via ATR. Thus, particularly high differences between import and export country energy cost (cheap hydrogen in export country and expensive electricity in import country) work in favor of ATR, as here almost all energy is required in the exporting country, whereas in the case of eSMR, a relevant share of total energy consumption occurs in the importing country.
- In order to enable a hydrogen supply that is climate-neutral, the CO_2 which is required for the conversion of hydrogen into SNG must be of non-fossil origin. One possible approach is to use the CO_2 within a closed cycle. A CO_2 supply by means of such a closed cycle potentially offers comparatively easy scalability, especially in comparison to the sole use of limited biogenic CO_2 sources. Whether the overall hydrogen supply cost can be reduced by using such a CO_2 cycle depends on various factors. The availability of a low-cost biogenic CO_2 source at the point-of-export and the transportation distance are of particular importance. From today's perspective, most likely such a CO_2 cycle leads to a cost reduction, if no biogenic CO_2 source is available at the point-of-export and the onsite supply would have to be realized via the DAC process. For a transportation distance of 10,000 km, for example, the specific cost of CO_2 cycling is around 60 $€_{2020}/kg_{CO2}$ and thus significantly below the cost to be expected for CO_2 supply with DAC.

Funding

This research did not receive any specific grant from funding agencies in the public, commercial, or not-for-profit sectors.

CRediT authorship contribution statement

Fabian Carels: Writing – original draft, Visualization, Validation, Methodology, Investigation, Data curation, Conceptualization. **Lucas Sens:** Writing – review & editing, Supervision, Methodology, Data curation. **Martin Kaltschmitt:** Writing – review & editing, Supervision, Conceptualization.

Declaration of competing interest

The authors declare that they have no known competing financial interests or personal relationships that could have appeared to influence the work reported in this paper.

Data availability

Data will be made available on request.

References

[1] Statista. Global LNG trade volume 1970-2022 | Statista. [August 10, 2024]; Available from: https://www.statista.com/statistics/264000/global-lng-trade-volume-since-1970/.
[2] Energy Institute. Statistical Review of World Energy | 2023; 2023.
[3] IEA. Medium-Term Gas Report 2023: Including the Gas Market Report, Q4-2023 2023.
[4] Global Energy Monitor. Global Gas Infrastructure Tracker. [August 10, 2024]; Available from: https://globalenergymonitor.org/projects/global-gas-infrastructure-tracker/tracker/.
[5] European Commission. Liquefied natural gas. [August 10, 2024]; Available from: https://energy.ec.europa.eu/topics/oil-gas-and-coal/liquefied-natural-gas_en.
[6] IEA. Gas Market Report Q1, 2023: including Gas Market Highlights 2022.
[7] IEA. Net Zero by 2050 - A Roadmap for the Global Energy Sector; 2021.
[8] IPCC. Climate Change 2022 – Impacts, Adaptation and Vulnerability. Cambridge University Press; 2023.
[9] Riemer M, Wachsmuth J. Conversion of LNG Terminals for Liquid Hydrogen: Analysis of Technical Feasibility under Economic Considerations; 2022.
[10] Bukold S. LNG-Terminals in Deutschland: Notwendiges Kriseninstrument oder Trojanisches Pferd der fossilen Gaswirtschaft?; 2022.
[11] Wettengel J. RWE aims to make LNG import terminal hydrogen-ready with green ammonia. [August 10, 2024]; Available from: https://www.cleanenergywire.org/news/rwe-aims-make-lng-import-terminal-hydrogen-ready-green-ammonia.
[12] Radowitz B. Uniper resumes plans for 'hydrogen-ready' German LNG terminal: Fortum CEO. [August 10, 2024]; Available from: https://www.rechargenews.com/energy-transition/uniper-resumes-plans-for-hydrogen-ready-german-lng-terminal-fortum-ceo/2-1-1179191.
[13] IEA. World Energy Outlook 2022; 2022.
[14] IRENA - International Renewable Energy Agency. Global hydrogen trade to meet the 1.5°C climate goal: Part I - Trade outlook for 2050 and way forward. International Renewable Energy Agency; 2022.
[15] Schühle P, Stöber R, Semmel M, Schaadt A, Szolak R, Thill S, et al. Dimethyl ether/CO 2 – a hitherto underestimated H 2 storage cycle. Energy Environ Sci 2023;16(7):3002–13. https://doi.org/10.1039/D3EE00228D.
[16] TES H2. Green Cycle | TES H2. [August 10, 2024]; Available from: https://tes-h2.com/green-cycle.
[17] Hampp J, Düren M, Brown T. Import options for chemical energy carriers from renewable sources to Germany. PLoS One 2023;18(2):e0262340.
[18] Ortiz Cebolla R, Dolci F, Weidner E. Assessment of Hydrogen Delivery Options. Publications Office of the European Union. https://doi.org/10.2760/869085.
[19] Staiß F, Schmidt M, Stephanos C, Stöcker P, Wurbs S. Optionen für den Import grünen Wasserstoffs nach Deutschland bis zum Jahr 2030. Materialband (Schriftenreihe Ener-; 2022.
[20] Lehner M, Tichler R, Steinmüller H, Koppe M. Power-to-Gas: Technology and Business Models. Springer; 2014.
[21] Pastor-Pérez L, Patel V, Le Saché E, Reina TR. CO2 methanation in the presence of methane: Catalysts design and effect of methane concentration in the reaction mixture. J Energy Inst 2020;93(1):415–24. https://doi.org/10.1016/j.joei.2019.01.015.
[22] Jürgensen L, Ehimen EA, Born J, Holm-Nielsen JB. Dynamic biogas upgrading based on the Sabatier process: thermodynamic and dynamic process simulation. Bioresour Technol 2015;178:323–9. https://doi.org/10.1016/j.biortech.2014.10.069.

[23] Schmidt M, Schwarz S, Stürmer B, Wagener l, Zuberbühler U. Technologiebericht 4.2a Power-to-gas (Methanisierung chemisch-katalytisch). In: Wuppertal Institut, Fraunhofer ISI, IZES, editor. Technologien für die Energiewende. Teilbericht 2 an das Bundesministerium für Wirtschaft und Energie (BMWi). Wuppertal, Karlsruhe, Saarbrücken; 2018.

[24] Brynolf S, Taljegard M, Grahn M, Hansson J. Electrofuels for the transport sector: a review of production costs. Renew Sustain Energy Rev 2018;81:1887–905. https://doi.org/10.1016/j.rser.2017.05.288.

[25] Peters R, Baltruweit M, Grube T, Samsun RC, Stolten D. A techno economic analysis of the power to gas route. J CO2 Util 2019;34:616–34. https://doi.org/10.1016/j.jcou.2019.07.009.

[26] Heß D, Klumpp M, Dittmeyer R. Nutzung von CO2 aus Luft als Rohstoff für synthetische Kraftstoffe und Chemikalien; 2020.

[27] Bajohr S. Power-to-gas Technologies: STORE&GO Workshop; 2020.

[28] Becker WL, Penev M, Braun RJ. Production of synthetic natural gas from carbon dioxide and renewably generated hydrogen: a techno-economic analysis of a power-to-gas strategy. J Energy Res Technol 2019;141(2). https://doi.org/10.1115/1.4041381.

[29] Adolf J, Balzer C, Kofod M, Lenz B, Lischke A, Knitschky G et al. Liquefied Natural Gas - New Energy for Ships and Trucks?: Facts, Trends and Perspectives. Shell LNG Study; 2019.

[30] Mokhatab S. Handbook of Liquefied Natural Gas. Burlington: Elsevier Science; 2013.

[31] Pospíšil J, Charvát P, Arsenyeva O, Klimeš L, Špiláček M, Klemeš JJ. Energy demand of liquefaction and regasification of natural gas and the potential of LNG for operative thermal energy storage. Renew Sustain Energy Rev 2019;99:1–15. https://doi.org/10.1016/j.rser.2018.09.027.

[32] IEA. Global Hydrogen Review 2022; 2022.

[33] Cultofsea - Maritime Knowledgebase. Gas Tanker - Types, Tanks, Reliquefaction & Cargo handling. [August 10, 2024]; Available from: https://cultofsea.com/tanker/gas-tanker-types-tanks-cargo/.

[34] Moon K, Chang D, Lee D, Myung-Bae K, Ahn H-J, Ha J-P. Comparison of Spherical and Membrane Large LNG Carriers in Terms of Cargo Handling; 2005.

[35] Sönmez E, Kekre S, Scheller-Wolf A, Secomandi N. Strategic analysis of technology and capacity investments in the liquefied natural gas industry. Eur J Oper Res 2013;226(1):100–14. https://doi.org/10.1016/j.ejor.2012.10.042.

[36] Al-Breiki M, Bicer Y. Comparative cost assessment of sustainable energy carriers produced from natural gas accounting for boil-off gas and social cost of carbon. Energy Rep 2020;6:1897–909. https://doi.org/10.1016/j.egyr.2020.07.013.

[37] He T, Chong ZR, Zheng J, Ju Y, Linga P. LNG cold energy utilization: prospects and challenges. Energy 2019;170:557–68. https://doi.org/10.1016/j.energy.2018.12.170.

[38] Wismann ST, Engbæk JS, Vendelbo SB, Eriksen WL, Frandsen C, Mortensen PM, et al. Electrified methane reforming: understanding the dynamic interplay. Ind Eng Chem Res 2019;58(51):23380–8. https://doi.org/10.1021/acs.iecr.9b04182.

[39] Baltac S, Wilson M, O'Sullivan C, Leguijt C, Beeftink, Mart: Nieuwenhuijse, Isabel. Low-Carbon hydrogen from Natural Gas: Global Roadmap; 2022.

[40] Parkinson B, Tabatabaei M, Upham DC, Ballinger B, Greig C, Smart S, et al. Hydrogen production using methane: Techno-economics of decarbonizing fuels and chemicals. Int J Hydrogen Energy 2018;43(5):2540–55. https://doi.org/10.1016/j.ijhydene.2017.12.081.

[41] IEA. The Future of Hydrogen; 2019.

[42] Parkinson B, Balcombe P, Speirs JF, Hawkes AD, Hellgardt K. Levelized cost of CO 2 mitigation from hydrogen production routes. Energy Environ Sci 2019;12(1):19–40. https://doi.org/10.1039/c8ee02079e.

[43] IEA. Global Hydrogen Review 2021; 2021.

[44] Pruvost F, Cloete S, Del Arnaiz PC, Zaabout A. Blue, green, and turquoise pathways for minimizing hydrogen production costs from steam methane reforming with CO2 capture. Energ Conver Manage 2022;274:116458. https://doi.org/10.1016/j.enconman.2022.116458.

[45] Oni AO, Anaya K, Giwa T, Di Lullo G, Kumar A. Comparative assessment of blue hydrogen from steam methane reforming, autothermal reforming, and natural gas decomposition technologies for natural gas-producing regions. Energ Conver Manage 2022;254:115245. https://doi.org/10.1016/j.enconman.2022.115245.

[46] Collodi G, Azzaro G, Ferrari N, Santos S. Techno-economic evaluation of deploying CCS in SMR based merchant H2 production with NG as feedstock and fuel. Energy Procedia 2017;114:2690–712. https://doi.org/10.1016/j.egypro.2017.03.1533.

[47] Tinoco RR, Bouallou C. Hydrogen production from natural gas: auto-thermal reforming and CO2 capture. Chem Eng Trans 2010. https://doi.org/10.3303/CET1021028.

[48] Ciambelli P. Catalytic autothermal reforming for hydrogen production: from large-scale plant to distributed energy system. In: van der Voorde M, editor. Hydrogen Production and Energy Transition. De Gruyter; 2021.

[49] Sadler D, Solgaard Anderson H, Sperrink, Martin, Cargill, Al. H21 North of England; 2018.

[50] H-vision. Blue hydrogen as accelerator and pioneer for energy transition in the industry: Feasibility study report; 2019.

[51] Wang A, Jens J, Mavins D, Moultak M, Schimmel M, van der Leun K et al. Analysing future demand, supply, and transport of hydrogen; 2021.

[52] Bailey M. Haldor Topsoe starts up sustainable methanol demonstration plant in Denmark. [August 10, 2024]; Available from: https://www.chemengonline.com/haldor-topsoe-starts-up-sustainable-methanol-demonstration-plant-in-denmark/.

[53] Haldor Topsoe. eREACT™ Hydrogen: The future of blue hydrogen | Equipment | Products | Topsoe. [August 10, 2024]; Available from: https://www.topsoe.com/our-resources/knowledge/our-products/equipment/ereact-hydrogen.

[54] Iaquaniello G, Palo E, Salladini A. An overview of today's industrial processes to make hydrogen and future developments' trend. In: van der Voorde M, editor. Hydrogen Production and Energy Transition. De Gruyter; 2021.

[55] Kreitz B, Biessey P, Börnhorst M, Schallhart V, Westermann T. Trendbericht technische chemie 2022. Nachr Chem 2022;70(4):56–64. https://doi.org/10.1002/nadc.20224124649.

[56] Korambath P, Wang J, Kumar A, Davis J, Graybill R, Schott B, et al. A smart manufacturing use case: furnace temperature balancing in steam methane reforming process via kepler workflows. Procedia Comput Sci 2016;80:680–9. https://doi.org/10.1016/j.procs.2016.05.357.

[57] Wismann ST, Engbæk JS, Vendelbo SB, Bendixen FB, Eriksen WL, Aasberg-Petersen K, et al. Electrified methane reforming: a compact approach to greener industrial hydrogen production. Science 2019;364(6442):756–9. https://doi.org/10.1126/science.aaw8775.

[58] Seo Y, Huh C, Lee S, Chang D. Comparison of CO_2 liquefaction pressures for ship-based carbon capture and storage (CCS) chain. Int J Greenhouse Gas Control 2016;52:1–12. https://doi.org/10.1016/j.ijggc.2016.06.011.

[59] Yara. New liquid CO2 ship for Yara. [August 10, 2024]; Available from: https://www.yara.com/news-and-media/news/archive/2015/new-liquid-co2-ship-for-yara/.

[60] Reyes-Lúa. Adriana, Arellano Y, Treu Røe I, Rycroft L, Wildenborg T, Jordal K. CO_2 ship transport: Benefits for early movers and aspects to consider: 4th Report of the Thematic Working Group on: CO2 Transport, Storage, and Networks; 2021.

[61] Durusut E, Joos M. Shipping CO2 - UK cost estimation study; 2018.

[62] Messer Group GmbH. Properties of Carbon Dioxide. [August 10, 2024]; Available from: https://elmemesser.ru/wp-content/uploads/sites/5/2020/08/CO2-EN-web.pdf.

[63] Orchard K, Durusut E, Skagestad R, Hay M, Ombudstvedt I. The Status and Challenges of CO2 Shipping Infrastructures; 2020.

[64] Al Baroudi H, Awoyomi A, Patchigolla K, Jonnalagadda K, Anthony EJ. A review of large-scale CO2 shipping and marine emissions management for carbon capture, utilisation and storage. Appl Energy 2021;287:116510. https://doi.org/10.1016/j.apenergy.2021.116510.

[65] Yoo B-Y, Choi D-K, Kim H-J, Moon Y-S, Na H-S, Lee S-G. Development of CO2 terminal and CO2 carrier for future commercialized CCS market. Int J Greenhouse Gas Control 2013;12:323–32. https://doi.org/10.1016/j.ijggc.2012.11.008.

[66] Schmidt P, Zittel W, Weindorf W, Raksha T. Renewables in Transport 2050: Empowering a sustainable mobility future with zero emission fuels from renewable electricity; 2016.

[67] Kramer U, Ortloff F, Thee R. Defossilisierung des Transportsektors: Optionen und Voraussetzungen. Deutschland 2018.

[68] Lowell D, Wang H, Lutsey N. Assessment of the fuel cycle impact of liquefied natural gas as used in international shipping; 2013.

[69] Pavlenko N, Comer B, Zhou Y, Clark N, Rutherford D. The climate implications of using LNG as a marine fuel; 2020.

[70] Ericsson K. Biogenic carbon dioxide as feedstock for production of chemicals and fuels: A techno-economic assessment with a European perspective. Lund: Miljö- och energisystem, LTH, Lunds universitet.

[71] Rodin V, Lindorfer J, Böhm H, Vieira L. Assessing the potential of carbon dioxide valorisation in Europe with focus on biogenic CO2. J CO2 Util 2020. https://doi.org/10.1016/j.jcou.2020.101219.

[72] Liebich A, et al. Detailanalysen zum Systemvergleich speicherbarer Energieträger aus erneuerbaren Energien: Anhang zum Abschlussbericht.

[73] Billig E. Bewertung technischer und wirtschaftlicher Entwicklungspotenziale künftiger und bestehender Biomasse-zu-Methan-Konversionsprozesse [Dissertation]. Leipzig: Universität Leipzig; Helmholtz-Zentrum für Umweltforschung.

[74] Reiter G, Lindorfer J. Evaluating CO2 sources for power-to-gas applications – a case study for Austria. J CO2 Util 2015;10:40–9. https://doi.org/10.1016/j.jcou.2015.03.003.

[75] Climeworks. Product Sheet CO2 Capture Plant.

[76] Keith DW, Holmes G, St. Angelo D, Heidel K. A Process for Capturing CO2 from the Atmosphere. Joule 2018;2(8):1573–94. https://doi.org/10.1016/j.joule.2018.05.006.

[77] Fasihi M, Efimova O, Breyer C. Techno-economic assessment of CO2 direct air capture plants. J Clean Prod 2019;224:957–80. https://doi.org/10.1016/j.jclepro.2019.03.086.

[78] IPCC. Climate Change 2021: The Physical Science Basis: Contribution of Working Group I to the Sixth Assessment Report of the Intergovernmental Panel on Climate Change. Cambridge University Press; 2023.

[79] EPA. Understanding Global Warming Potentials. [October 25, 2023]; Available from: https://www.epa.gov/ghgemissions/understanding-global-warming-potentials.

[80] Raab M, Maier S, Dietrich R-U. Comparative techno-economic assessment of a large-scale hydrogen transport via liquid transport media. Int J Hydrogen Energy 2021;46(21):11956–68. https://doi.org/10.1016/j.ijhydene.2020.12.213.

[81] Kamiya S, Nishimura M, Harada E. Study on introduction of CO2 free energy to japan with liquid hydrogen. Phys Procedia 2015;67:11–9. https://doi.org/10.1016/j.phpro.2015.06.004.

[82] Srettiwat N, Safari M, Olcay H, Malina R. A techno-economic evaluation of solar-powered green hydrogen production for sustainable energy consumption in

Belgium. Int J Hydrogen Energy 2023. https://doi.org/10.1016/j.ijhydene.2023.09.159.

[83] Board of Governors of the Federal Reserve System. June 16, 2021: FOMC Projections materials, accessible version. [August 10, 2024]; Available from: https://www.federalreserve.gov/monetarypolicy/fomcprojtabl20210616.htm.

[84] European Central Bank. Economic bulletin. [August 10, 2024]; Available from: https://www.ecb.europa.eu/pub/economic-bulletin/html/index.en.html.

[85] European Commission. Commission Delegated Regulation (EU) 2023/1185; 2023.

[86] Umweltbundesamt. Treibhausgaspotentiale (Global Warming Potential, GWP) ausgewählter Verbindungen und deren Gemische gemäß Viertem (AR4) und Fünftem (AR5) Sachstandsbericht des IPCC bezogen auf einen Zeitraum von 100 Jahren; 2022.

[87] Sens L, Piguel Y, Neuling U, Timmerberg S, Wilbrand K, Kaltschmitt M. Cost minimized hydrogen from solar and wind – Production and supply in the European catchment area. Energ Conver Manage 2022;265:115742. https://doi.org/10.1016/j.enconman.2022.115742.

[88] Reuß M, Grube T, Robinius M, Stolten D. A hydrogen supply chain with spatial resolution: comparative analysis of infrastructure technologies in Germany. Appl Energy 2019;247:438–53. https://doi.org/10.1016/j.apenergy.2019.04.064.

[89] Arrigoni A, Bravo Diaz L. Hydrogen emissions from a hydrogen economy and their potential global warming impact: Summary report of the Clean Hydrogen Joint Undertaking Expert Workshop on the Environmental Impacts of Hydrogen; 2022.

[90] Department of Energy. Multi-Year Research, Development, and Demonstration Plan: 3.2 Hydrogen Delivery; 2015.

[91] Billig E, Decker M, Benzinger W, Ketelsen F, Pfeifer P, Peters R, et al. Non-fossil CO2 recycling—The technical potential for the present and future utilization for fuels in Germany. J CO2 Util 2019;30:130–41. https://doi.org/10.1016/j.jcou.2019.01.012.

[92] Vos M, Douma J, van den Noort A. Study on the import of liquid renewable energy: technology cost. Assessment 2020.

[93] Fasihi M, Bogdanov D, Breyer C. Long-Term Hydrocarbon Trade Options for the Maghreb Region and Europe—Renewable Energy Based Synthetic Fuels for a Net Zero Emissions World. Sustainability 2017;9(2):306.

[94] IRENA - International Renewable Energy Agency. Global hydrogen trade to meet the 1.5 °C climate goal: Part II - Technology review of hydrogen carriers; 2022.

[95] Pawelec G. Comparative report on alternative fuels for ship propulsion: System-based solutions for H2-fuelled water transport in North-West Europe; 2020.

[96] Timmerberg S, Bullerdiek N, Kaltschmitt M, Gnann T, Neumann F, Wietschel M. Teilstudie Import von Stromkraftstoffen für den Verkehr – Lkw, Binnen-Seeschiffe, Flugzeuge; 2018.

[97] Aspelund A, Jordal K. Gas conditioning—The interface between CO2 capture and transport. Int J Greenhouse Gas Control 2007;1(3):343–54. https://doi.org/10.1016/S1750-5836(07)00040-0.

[98] Fasihi M, Breyer C. Baseload electricity and hydrogen supply based on hybrid PV-wind power plants. J Clean Prod 2020;243:118466. https://doi.org/10.1016/j.jclepro.2019.118466.

[99] MAN Energy Solutions. Managing methane slip; 2020.

[100] Jeon SH, Choi YU, Kim MS. Review on boil-off gas (BOG) re-liquefaction system of liquefied CO 2 transport ship for carbon capture and sequestration (CCS). Int J Air-Cond Ref 2016;24(03):1650017. https://doi.org/10.1142/S2010132516500176.

[101] Teichmann D, Arlt W, Wasserscheid P. Liquid organic hydrogen carriers as an efficient vector for the transport and storage of renewable energy. Int J Hydrogen Energy 2012;37(23):18118–32. https://doi.org/10.1016/j.ijhydene.2012.08.066.

[102] Niermann M, Timmerberg S, Drünert S, Kaltschmitt M. Liquid organic hydrogen carriers and alternatives for international transport of renewable hydrogen. Renew Sustain Energy Rev 2021;135:110171. https://doi.org/10.1016/j.rser.2020.110171.

[103] Hurskainen M. Liquid organic hydrogen carriers (LOHC). Concept Evaluation and Techno-economics 2019.

[104] Lauri K, Jouko R, Nicklas N, Sebastian T. Scenarios and new technologies for a North-European CO2 transport infrastructure in 2050. Energy Procedia 2014;63:2738–56. https://doi.org/10.1016/j.egypro.2014.11.297.

[105] Mletzko J, Ehlers S, Kather A. Comparison of natural gas combined cycle power plants with post combustion and oxyfuel technology at different CO2 capture rates. Energy Procedia 2016;86:2–11. https://doi.org/10.1016/j.egypro.2016.01.001.

[106] Kriegel R. Dezentrale Sauerstoffproduktion; 2022.

[107] Beysel G. Enhanced Cryogenic Air Separation: A proven Process applied to Oxyfuel. Cottbus; 2009.

[108] Radgen P, Cremer C, Warkentin S, Gerling P, May F, Knopf S. Verfahren zur CO2 Abscheidung und –Speicherung. Zusammenfassung 2006.

[109] Parks G. Hydrogen station compression, storage, and dispensing technical status and costs. Indep Rev 2014. https://doi.org/10.13140/RG.2.2.23768.34562.

[110] Reuß M, Grube T, Robinius M, Preuster P, Wasserscheid P, Stolten D. Seasonal storage and alternative carriers: a flexible hydrogen supply chain model. Appl Energy 2017;200:290–302. https://doi.org/10.1016/j.apenergy.2017.05.050.

[111] Nexant et al. Hydrogen Delivery Infrastructure Analysis: Interim Report; 2008.

[112] Sterchele Pea. Wege zu einem klimaneutralen Energiesystem: Die deutsche Energiewende im Kontext gesellschaftlicher Verhaltensweisen; 2020.

[113] Luderer G, Kost C, Sörgel D. Deutschland auf dem Weg zur Klimaneutralität 2045 - Szenarien und Pfade im Modellvergleich. Potsdam Institute for Climate Impact Research 2021.